Spectrum Usage Models for the Analysis, Design and Simulation of Cognitive Radio Networks

Index terms: cognitive radio, dynamic spectrum access, spectrum models.

Table of contents

1. Introduction

The dynamic spectrum access (DSA) principle based on the cognitive radio (CR) paradigm has been identified as a promising solution to conciliate the conflicts between the ever-increasing spectrum demand growth and the demonstrated spectrum underutilisation in legacy wireless communication systems. The basic underlying idea of DSA/CR is to allow unlicensed (secondary) users to access in an opportunistic and non-interfering manner some licensed bands temporarily unoccupied by the licensed (primary) users. Unlicensed secondary terminals sense the spectrum to detect spectrum gaps in the spectral activity patterns of the primary users, opportunistically transmit on them and vacate the channel as soon as a primary user reappears in the channel. Secondary unlicensed transmissions following this operating principle are allowed provided that no harmful interference is caused to the licensed primary system.

The existing DSA/CR techniques have commonly been envisaged, designed, developed and evaluated by means of analytical studies and computer simulations, which unavoidably rely on assumptions and models required to describe and characterise certain aspects of the system and scenario under study. The purpose of such models is to simplify some parts of the real environment in order to provide a tractable, yet realistic representation thereof that can adequately be employed in analytical studies or implemented in simulation tools for the performance evaluation of DSA/CR techniques. Due to the opportunistic nature of the DSA/CR principle, the behaviour and performance of a secondary network depends on the spectrum occupancy patterns of the primary system. A realistic and accurate modelling of such patterns becomes therefore essential and extremely useful in the domain of the DSA/CR technology. The potential applicability of spectrum usage models ranges from analytical studies to the design and dimensioning of DSA/CR networks as well as the development of innovative simulation tools and more efficient DSA/CR techniques.

The modelling of spectrum usage for the study of radio communication systems has been an important concern for several decades. Early models and studies on spectrum usage date from the late 1970s, when the usage patterns in the high frequency (HF) band were analysed and characterised [1][2]. However, the unique features of DSA/CR systems, bands of operation and modern primary radio communication systems lead to a particularly complex scenario that requires tailored modelling approaches [3]. This chapter presents a comprehensive set of spectrum occupancy models specifically envisaged for the analysis, design and simulation of DSA/CR systems. The models described in this chapter have been proven to accurately capture and reproduce the relevant statistical properties of spectrum usage in real wireless communication systems. Based on the particular set of statistical properties and features taken into account, spectrum models can be categorised into time-, frequency- and space-dimension models, which are discussed in Sections 2-4, respectively. The combination and joint integration of the existing models into a unified modelling approach is discussed in Section 5. Finally, Section 6 provides some concluding remarks.

2. Time-dimension models

At a given time instant, a primary radio channel may be either busy or idle. Hence, from the point of view of a DSA/CR system, the time occupancy pattern of a primary radio channel can adequately be modelled by means of a two-state Markov chain. The state space for a primary radio channel can be denoted by $\mathbb{S} = \{s_0, s_1\}$, where the s_0 state indicates that the channel is idle (i.e., available for secondary use) and the s_1 state indicates that the channel is busy (i.e., used by a primary user and therefore not available for opportunistic access). The channel state $S(t)$ at time t can be either $S(t) = s_0$ or $S(t) = s_1$. The Markov chain model may be discrete or continuous depending on the time index set t. The particular characteristics of each case are discussed in the following subsections.

2.1. Discrete-time models

2.1.1. Stationary DTMC model

In the Discrete-Time Markov Chain (DTMC) model, the time index set is discrete (i.e., $t = t_k = kT_s$, where k is a non-negative integer representing the step number and T_s is the time period between consecutive transitions or state changes). According to this model, the channel remains in a certain state at each step, with the state changing randomly between steps. The behaviour of the channel is described by means of a set of transition probabilities between states as depicted in Figure 1. The transition probabilities can be expressed in matrix form as:

$$\mathbf{P} = \begin{bmatrix} p_{00} & p_{01} \\ p_{10} & p_{11} \end{bmatrix} \tag{1.1}$$

where p_{ij} represents the probability that the system transitions from state s_i to state s_j. In its simplest form, the transition matrix $\mathbf{P}$ may be assumed to be constant and independent of the time instant t, in which case the DTMC is said to be *stationary* or *time-homogeneous*.

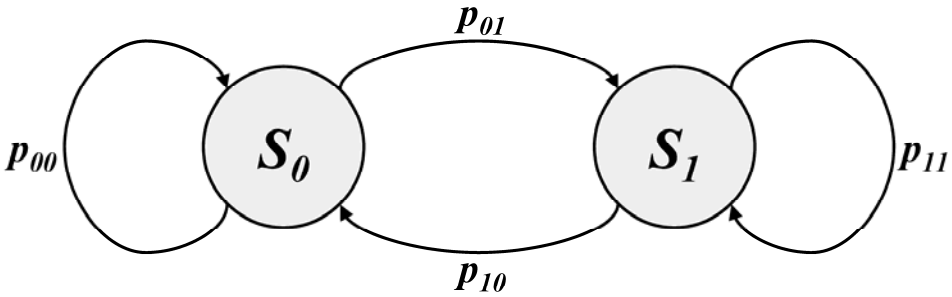

Figure 1 Discrete-Time Markov Chain (DTMC) model.

The duty cycle (DC) of a channel, henceforth denoted by Ψ, is a very straightforward metric and an accurate reproduction is a minimum requirement for any time-dimension model of spectrum usage. The DC can be defined as the probability that the channel is busy. The probabilities that the model of Figure 1 is in each of its states in the long term are given by [4]:

$$\begin{aligned} P(S = s_0) &= \frac{p_{10}}{p_{01} + p_{10}} = 1 - \Psi \\ P(S = s_1) &= \frac{p_{01}}{p_{01} + p_{10}} = \Psi \end{aligned} \tag{1.2}$$

Thus, the DTMC model can be configured to reproduce any arbitrary DC, Ψ, by selecting the transition probabilities as $p_{01} = p_{11} = \Psi$ and $p_{10} = p_{00} = 1 - \Psi$, which yields:

$$\mathbf{P} = \begin{bmatrix} 1-\Psi & \Psi \\ 1-\Psi & \Psi \end{bmatrix} \tag{1.3}$$

Nevertheless, reproducing not only the DC of a channel but also the lengths of the busy and idle periods is an important characteristic of a realistic time-dimension model of spectrum usage. In the case of the DTMC model, however, there is no means to account for this feature and, as such, the model is not able to reproduce, in general, this property of spectrum usage. This is illustrated in

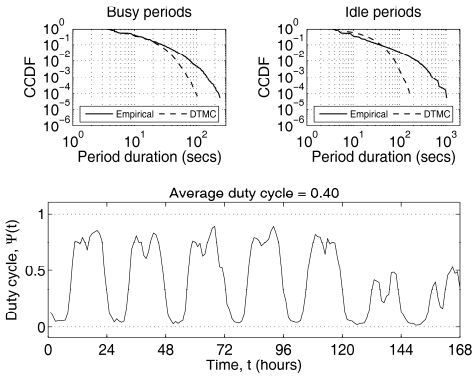

Figure 2 Empirical and DTMC-simulated distributions of busy and idle periods along with DC time evolution for a DCS 1800 downlink channel.

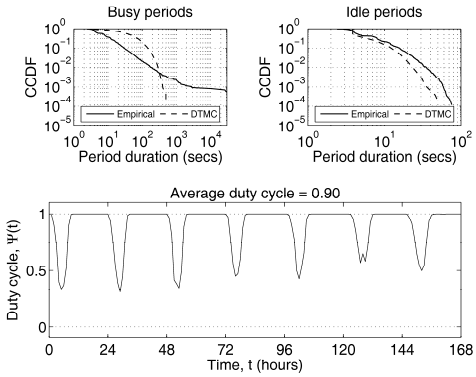

Figure 3 Empirical and DTMC-simulated distributions of busy and idle periods along with DC time evolution for an E-GSM 900 downlink channel.

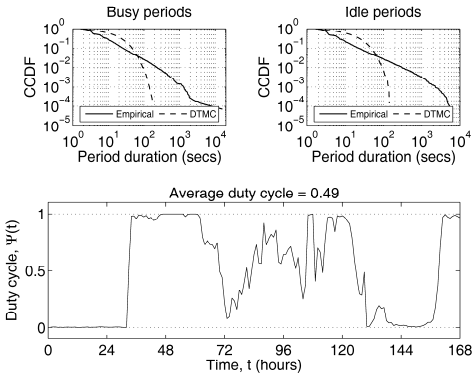

Figure 4 Empirical and DTMC-simulated distributions of busy and idle periods along with DC time evolution for a TETRA downlink channel.

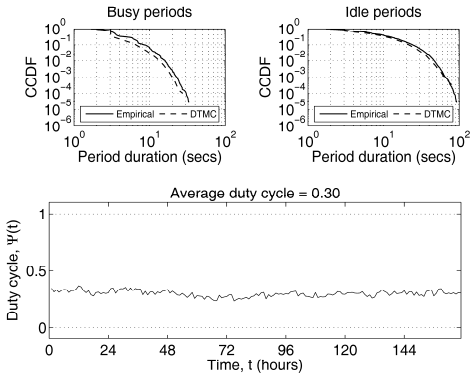

Figure 5 Empirical and DTMC-simulated distributions of busy and idle periods along with DC time evolution for a TETRA uplink channel.

Figure 2, Figure 3, Figure 4 and Figure 5, which show the empirical distributions, in terms of the complementary cumulative distribution function (CCDF), for the lengths of busy and idle periods of some selected real channels along with the corresponding distributions obtained by means of simulation with the stationary DTMC channel model of Figure 1 (the transition probabilities are extracted from the channel occupancy patterns). The capability of the DTMC model to reproduce the statistical distributions of busy and idle periods in real channels can be explained based on the load variation pattern of the channel, which is also shown in Figure 2, Figure 3, Figure 4 and Figure 5 in terms of the DC. When the channel is sparsely used (i.e., the load/DC is low), the length of idle periods is significantly higher than that of busy periods. On the other hand, when the channel is subject to an intensive usage (i.e., the load/DC is high), the length of busy periods increases while idle periods become notably shorter. Since the stationary DTMC model is parameterised (i.e., the transition probabilities are configured) based on the long-term average load of the channel (i.e., the average DC), it is not able to capture the channel load variations. As a result, the stationary DTMC model cannot reproduce the resulting lengths of busy and idle periods as appreciated in Figure 2, Figure 3 and Figure 4, where the channel load varies over time and the distributions obtained by simulation diverge from the real ones. The exception corresponds to the case of channels with constant load patterns, where the average channel load matches the instantaneous load at all times, and the empirical and simulation results agree as observed in Figure 5. Therefore, the stationary DTMC model can be an appropriate modelling approach for channels with a constant load level that does not change significantly over time, as it is the case of the example shown in Figure 5. If the channel load shows some variation pattern as in Figure 2, Figure 3 and Figure 4, other modelling approaches, as discussed in Section 2.1.2, are more convenient.

2.1.2. Non-stationary DTMC model

For channels with varying load patterns the DC changes over time, meaning that the probabilities of the transition matrix $\mathbf{P}$ are also time-variant. In such a case, a *non-stationary* or *time-inhomogeneous* DTMC needs to be considered, with a time-dependent transition matrix:

$$\mathbf{P}(t) = \begin{bmatrix} 1-\Psi(t) & \Psi(t) \\ 1-\Psi(t) & \Psi(t) \end{bmatrix} \tag{1.4}$$

where $t = t_k = kT_s$. In the stationary case of equation (1.3), Ψ represents a constant parameter. However, in the non-stationary case of equation (1.4), $\Psi(t)$ represents a time-dependent function that needs to be characterised in order to characterise the complete DTMC channel model in the time domain [5]. Figure 2, Figure 3, Figure 4 indicate the existence of two well-defined types of channel load variation patterns, namely patterns with an important and remarkably predominant deterministic component (i.e., Figure 2 and Figure 3) and patterns where the carried load appears to vary following a random behaviour (i.e., Figure 4). Adequate DC models of $\Psi(t)$ for both cases are presented in Sections 2.1.2.1 and 2.1.2.2 following deterministic and stochastic modelling approaches, respectively.

2.1.2.1. Deterministic duty cycle models

In certain cases, the load variation patterns of primary radio channels are characterised by a predominant deterministic component arising from social behaviour and common habits, as in Figure 2 and Figure 3. These examples correspond to cellular mobile communication systems, namely the Global System for Mobile communications (GSM) operating in the 900-MHz band and its counterpart in the 1.8-GHz band, the Digital Cellular System (DCS). Similar patterns can also be present in other cellular technologies such as the TErrestrial Trunked Radio (TETRA) system.

The load variation pattern of a cellular mobile communication system can be described by means of Auto-Regressive Integrated Moving Average (ARIMA) time series models [6]. This section presents an alternative modelling approach based on the observation that the time evolution of $\Psi(t)$ over time periods of certain length exhibits a clear and predominant deterministic component. In particular, Figure 2 and Figure 3 indicate that the variation pattern of $\Psi(t)$ is periodic with a period of one day (24 hours) and a slightly different shape between weekdays and weekends due to the lower traffic load normally associated with weekends. Two different shapes for $\Psi(t)$ can be identified. The first shape type is normally present in channels with low/medium loads (average DCs) as in the example of Figure 2, while the second shape type is more commonly observed in channels with medium/high loads as in the example of Figure 3 [7].

For channels with low/medium load (see Figure 2), the shape of $\Psi(t)$ can be approximated by the summation of M bell-shaped exponential terms centred at time instants τ_m, with amplitudes A_m and widths σ_m:

$$\Psi(t) \approx \Psi_{min} + \sum_{m=0}^{M-1} A_m e^{-\left(\frac{t-\tau_m}{\sigma_m}\right)^2}, \quad 0 \le t \le T \tag{1.5}$$

where $\Psi_{min} = \min\{\Psi(t)\}$ and T is the time interval over which $\Psi(t)$ is periodic (i.e., one day).

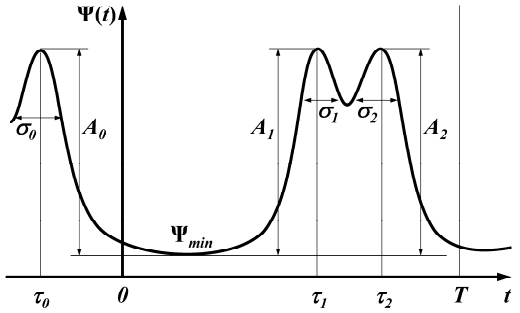

Figure 6 Parameters of the deterministic duty cycle model for low/medium loads.

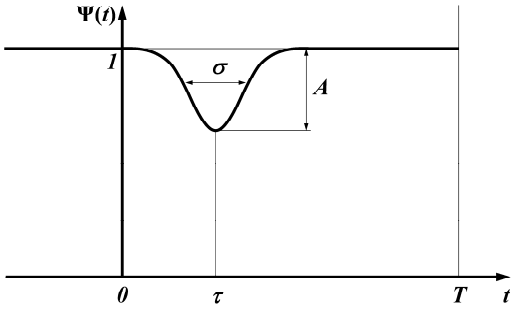

Figure 7 Parameters of the deterministic duty cycle model for medium/high loads.

The analysis of empirical data indicates that $\Psi(t)$ can accurately be described by means of $M=3$ terms with τ_1 and τ_2 corresponding to *busy hours* and $\tau_0=\tau_2-T$ as illustrated in Figure 6. Moreover, the approximations $A_0=A_1=A_2=A$ and $\sigma_0=\sigma_1=\sigma_2=\sigma$ are acceptable without incurring in excessive errors, which simplifies the model:

$$\Psi(t)\approx\Psi_{min}+A\sum_{m=0}^{M-1}e^{-\left(\frac{t-\tau_m}{\sigma}\right)^2},\quad 0\le t\le T \tag{1.6}$$

Notice that A determines the average value of $\Psi(t)$ in the time interval $[0,T]$, denoted by $\overline{\Psi}$, and it can therefore be expressed as a function of $\overline{\Psi}$ taking into account that:

$$\overline{\Psi}=\frac{1}{T}\int_0^T\Psi(t)dt\approx\Psi_{min}+\frac{A}{T}\sum_{m=0}^{M-1}\int_0^T e^{-\left(\frac{t-\tau_m}{\sigma}\right)^2}dt \tag{1.7}$$

Solving equation (1.7) for A yields:

$$A=\left(\overline{\Psi}-\Psi_{min}\right)T\left[\sum_{m=0}^{M-1}\int_0^T e^{-\left(\frac{t-\tau_m}{\sigma}\right)^2}dt\right]^{-1} \tag{1.8}$$

Substituting equation (1.8) in equation (1.6) and solving the integral yields the DC model:

$$\Psi(t)\approx\Psi_{min}+\frac{2T\left(\overline{\Psi}-\Psi_{min}\right)}{\sigma\sqrt{\pi}}\cdot\frac{f_{\exp}^{1/m}(t,\tau_m,\sigma)}{f_{\mathrm{erf}}^{1/m}(T,\tau_m,\sigma)} \tag{1.9}$$

where $\overline{\Psi}\ge\Psi_{min}$ \$ and:

$$\begin{aligned} f_{\exp}^{1/m}(t,\tau_m,\sigma) &= \sum_{m=0}^{M-1}e^{-\left(\frac{t-\tau_m}{\sigma}\right)^2} \\ f_{\mathrm{erf}}^{1/m}(T,\tau_m,\sigma) &= \sum_{m=0}^{M-1}\left[\mathrm{erf}\left(\frac{\tau_m}{\sigma}\right)+\mathrm{erf}\left(\frac{T-\tau_m}{\sigma}\right)\right] \end{aligned} \tag{1.10}$$

For channels with medium/high load (see Figure 3), the shape of $\Psi(t)$ can be approximated by an expression based on a single bell-shaped exponential term centred at time instant τ, with amplitude A and width σ:

$$\Psi(t) \approx 1 - Ae^{-\left(\frac{t-\tau}{\sigma}\right)^2}, \quad 0 \le t \le T \tag{1.11}$$

where T is the time interval over which $\Psi(t)$ is periodic (i.e., one day). The model is illustrated in Figure 7, with τ corresponding to the time with the lowest activity levels.

As in the previous case, A determines the average value of $\Psi(t)$ in the time interval $[0,T]$ and it can therefore be expressed as a function of $\overline{\Psi}$ taking into account that:

$$\overline{\Psi} = \frac{1}{T}\int_0^T \Psi(t)dt \approx 1 - \frac{A}{T}\int_0^T e^{-\left(\frac{t-\tau}{\sigma}\right)^2} dt \tag{1.12}$$

Solving equation (1.12) for A yields:

$$A = \left(1-\overline{\Psi}\right)T\left[\int_0^T e^{-\left(\frac{t-\tau}{\sigma}\right)^2} dt\right]^{-1} \tag{1.13}$$

Substituting equation (1.13) in equation (1.11) and solving the integral yields the DC model:

$$\Psi(t) \approx 1 - \frac{2T\left(1-\overline{\Psi}\right)}{\sigma\sqrt{\pi}} \cdot \frac{f_{\text{exp}}^{m/h}(t,\tau,\sigma)}{f_{\text{erf}}^{m/h}(T,\tau,\sigma)} \tag{1.14}$$

where:

$$f_{\text{exp}}^{m/h}(t,\tau,\sigma) = e^{-\left(\frac{t-\tau}{\sigma}\right)^2}$$

$$f_{\text{erf}}^{m/h}(T,\tau,\sigma) = \text{erf}\left(\frac{\tau}{\sigma}\right) + \text{erf}\left(\frac{T-\tau}{\sigma}\right)$$

The DC ranges within which each model is valid depends on the particular set of values selected for the configuration parameters. As a rough approximation, the DC model for low/medium loads can be valid for average DC values up to $\overline{\Psi} \approx 0.70$, while the DC model for medium/high loads can be valid down to $\overline{\Psi} \approx 0.45$. Any set of values for the model parameters can be valid as long as $\Psi(t)$ is confined within the interval $[0,1]$.

The capability of the non-stationary DTMC model along with the deterministic DC models to reproduce the statistical distributions of busy and idle periods in real channels is illustrated in Figure 8 and Figure 9, which are a reproduction of Figure 2 and Figure 3, respectively, including the distributions of busy and idle periods obtained by means of simulation with the non-stationary DTMC channel model. As it can be appreciated, the deterministic DC models are able to closely follow and reproduce the deterministic component of $\Psi(t)$ in the time domain and, as a result, the overall model is able to reproduce not only the mean DC of the channel, $\overline{\Psi}$, but also the statistical properties of busy and idle periods, which is not the case of the stationary DTMC model.

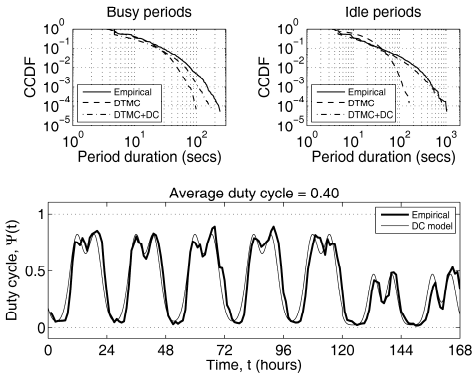

Figure 8 Empirical and DTMC-simulated distributions of busy and idle periods along with DC time evolution for a DCS 1800 downlink channel.

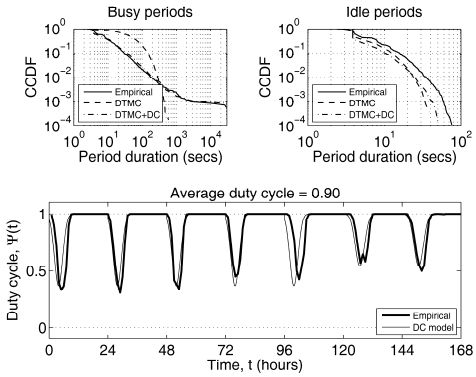

Figure 9 Empirical and DTMC-simulated distributions of busy and idle periods along with DC time evolution for a DCS 1800 downlink channel.

The presented DC models are envisaged to reproduce the deterministic pattern normally observed in cellular mobile communication systems such as E-GSM 900 and DCS 1800, which may also be present in other systems. Nevertheless, this does not imply that the model is always applicable to such type of systems. If the system is studied over relatively short time periods (e.g., a few hours), social behaviour and external events, which may not be easily predicted, may have a significant short-term impact on the channel usage. This may cause the deterministic component of $\Psi(t)$ to loss importance with respect to the random component and, as a result, the occupancy of a channel may experience high and unpredictable variations (e.g., see [8]). In such a case, deterministic DC models may be no longer valid and stochastic modelling approaches may constitute a more appropriate alternative.

2.1.2.2. Stochastic duty cycle models

The traffic load experienced in a radio channel is the consequence of a significant number of random factors such as the number of incoming and outgoing users, the resource management policies employed in the system, and so forth. Therefore, the channel usage level, represented by means of $\Psi(t)$, is itself a random variable (see Figure 4). As such, $\Psi(t)$ can be described and characterised by its probability density function (PDF). The empirical PDFs of $\Psi(t)$ in real systems can accurately be fitted with the beta distribution [9] and the Kumaraswamy distribution [10]. The PDF for the former is given by:

$$f_x^B(x;\alpha,\beta) = \frac{1}{B(\alpha,\beta)} x^{\alpha-1}(1-x)^{\beta-1}, \quad x \in (0,1) \tag{1.15}$$

where $\alpha > 0$ and $\beta > 0$ are shape parameters and $B(\alpha,\beta)$ is the beta function:

$$B(\alpha,\beta) = \int_0^1 z^{\alpha-1}(1-z)^{\beta-1} dz \tag{1.16}$$

while the PDF for the latter is given by:

$$f_x^K(x;a,b) = abx^{a-1}(1-x^a)^{b-1}, \quad x \in (0,1) \tag{1.17}$$

where $a > 0$ and $b > 0$ are shape parameters.

The beta distribution is a well-known and widely used distribution that can be found in many popular software simulation packages, thus facilitating the implementation of the stochastic DC model in simulation tools. However, it might present some difficulties in analytical studies due to the complex expression of its PDF. The Kumaraswamy distribution is similar to the beta distribution, but much simpler to use in analytical studies due to the simpler closed form of its PDF [11]. Therefore, while the former may be more appropriate for simulations, the latter may be more convenient for analytical studies.

Both distributions can be configured to reproduce any arbitrary mean DC, $\overline{\Psi}$, by properly selecting the distribution's parameters. In particular, the mean values of the beta and Kumaraswamy distributions are related with their shape parameters as [9][11]:

$$\overline{\Psi} = \begin{cases} \dfrac{\alpha}{\alpha+\beta} & \text{for beta distribution} \\ \\ bB\left(1+\dfrac{1}{a}, b\right) & \text{for Kumaraswamy distribution} \end{cases} \tag{1.18}$$

with $B(\alpha,\beta)$ given by equation (1.16). Notice that equation (1.18) can be satisfied for a given $\overline{\Psi}$ with different combinations of shape parameters α,β and a,b. The particular selection of the shape parameters determines the shape of the distributions as well as the resulting channel occupancy pattern in the time domain. The possible PDF shapes can be classified into six elemental archetypes, each with a characteristic time-domain pattern. Each archetype is defined by its load level (L: low, M: medium, and H: high) as well as its load pattern (type I: very bursty, and type II: moderately bursty, but not constant). The ranges of shape parameters for each archetype are related to the corresponding time-domain patterns as follows:

- Case L.I ($\alpha<1$, $\beta\geq 1$): The channel is used ($\Psi(t)>0$) sporadically and remains unused ($\Psi(t)\approx 0$) most of the time.
- Case L.II ($1<\alpha<\beta$): The channel is used ($\Psi(t)>0$) regularly by traffic with low activity factors.
- Case M.I ($\alpha<1$, $\beta<1$): The channel is subject to an intermittent use, where high-load periods are followed by low-load periods in a similar proportion.
- Case M.II ($\alpha>1$, $\beta>1$, $\alpha\sim\beta$): The channel usage level oscillates weakly around the average level.
- Case H.I ($\alpha\geq 1$, $\beta<1$): The channel is used ($\Psi(t)\approx 1$) most of the time, with some periods of lower occupancy levels ($\Psi(t)<1$).
- Case H.II ($\alpha>\beta>1$): The channel is not fully used ($\Psi(t)<1$) but subject to a constant, intensive usage.

The range of values indicated for the parameters of the beta distribution is also valid for the Kumaraswamy distribution by replacing α with a and β with b in type-I cases. In type-II cases, the resulting Kumaraswamy distribution is more difficult to control since the same constraints on a and b may hold for various load levels. Figure 10 and Figure 11 show some examples of the shape of the distributions and the resulting channel occupancy patterns in the time domain for channels with medium loads. Based on the above archetypes and the corresponding range of shape parameters, along with equation (1.18), the parameters of the models can be configured in order to reproduce not only arbitrary mean load levels but also a wide range of occupancy patterns.

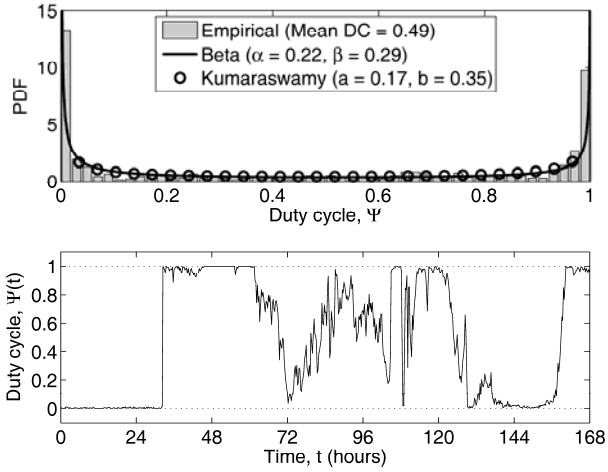

Figure 10 Stochastic DC models: case M.I.

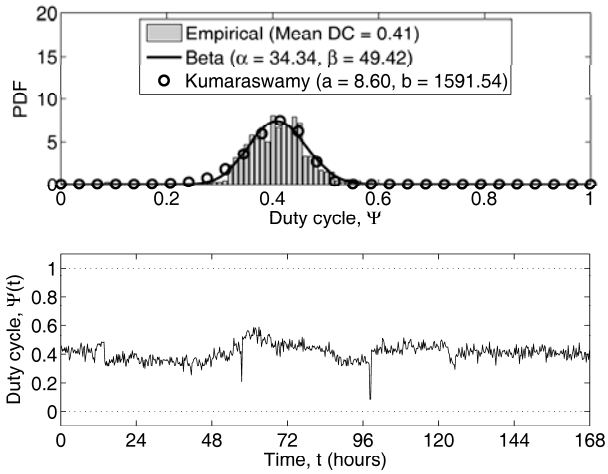

Figure 11 Stochastic DC models: case M.II.

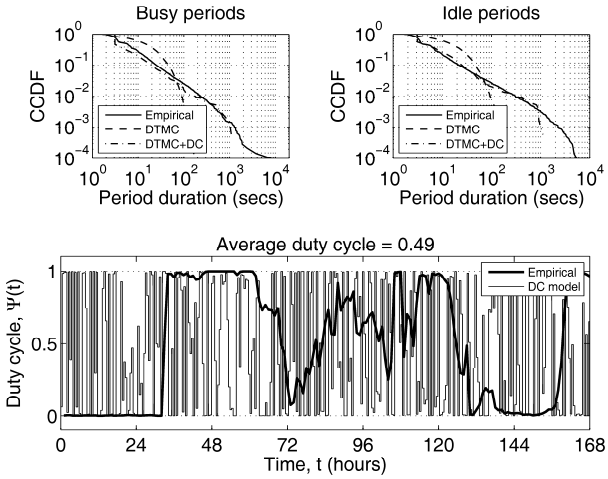

Figure 12 Empirical and DTMC-simulated distributions of busy and idle periods along with DC time evolution for a TETRA downlink channel.

The capability of the non-stationary DTMC model along with the stochastic DC models to reproduce the statistical distributions of busy and idle periods in real channels is illustrated in Figure 12, which is a reproduction of Figure 4 including the distributions of busy and idle periods obtained by means of simulation with the non-stationary DTMC channel model. As it can be appreciated, the sequence of $\Psi(t)$ values generated with the stochastic DC model does not follow the empirical $\Psi(t)$ values of the channel in the time domain. However, it is important to note that the stochastic approach is not aimed at reproducing the time evolution of a particular realisation of the stochastic process $\Psi(t)$, but the statistical properties thereof. The results shown in Figure 12 indicate that this is a valid and accurate modelling approach for channels with random load variation patterns.

When implemented in simulation tools, the non-stationary DTMC with stochastic DC models may not lead to accurate results if some observations are not carefully taken into account. In particular, the DTMC has to be iterated for a sufficient number of times, N, before updating the transition matrix $\mathbf{P}(t)$ according to the stochastic DC model. During such amount of iterations, the transition probabilities of the DTMC must remain unaltered. After N iterations, a new value of $\Psi(t)$ can be generated from a beta or Kumaraswamy distribution, and used to update the transition matrix $\mathbf{P}(t)$ for the next N iterations. If the transition matrix is updated excessively fast (e.g., every iteration) the overall model may not be able to accurately reproduce the lengths of busy and idle periods.

In summary, the non-stationary DTMC model along with the presented deterministic and stochastic DC models is able to accurately reproduce not only the mean occupancy level but also the statistical properties of busy and idle periods observed in real channels with varying load patterns.

2.2. Continuous-time models

In the Continuous-Time Markov Chain (CTMC) model, the time index set is continuous. According to this model, the channel remains in one state for a random time period before switching to the other state. The *state holding time* or *sojourn time* is modelled in the CTMC as an exponentially distributed random variable. Although the CTMC model has been widely employed in the domain of DSA/CR, some works based on field measurements have demonstrated that the state holding times are not exponentially distributed in real wireless communication systems. In particular, it has been found that state holding times are more adequately described by means of generalised Pareto [12], a mixture of uniform and generalised Pareto [13][14], hyper-Erlang [13][14], generalised Pareto and hyper-exponential [15] as well as geometric and log-normal [16] distributions. Based on these results, a more appropriate model is therefore the Continuous-Time Semi-Markov Chain (CTSMC) model, where the state holding times can follow any arbitrary distribution.

The probability distribution that better describes the length of busy and idle periods for a primary radio channel depends not only on the particular primary radio technology but also on the periodicity (time-resolution) at which the channel state is observed. On the one hand, observing the channel state at high sampling rates enables the true channel occupancy patterns to be extracted with high time accuracies. On the other hand, observing the channel state at low effective sampling rates with respect to the channel variation dynamics may result in a significant under-sampling, meaning that the true channel state may change between two consecutive channel observations. The occupancy pattern observed in such a case, although inaccurate, is interesting since it can be thought of as the perception of a DSA/CR user that periodically senses the channel and observes its state at discrete time instants. High time-resolution models are useful to accurately describe the true channel occupancy pattern at short time scales. Low time-resolution models are useful as well to characterise the spectrum occupancy from the point of view of the DSA/CR user perception (i.e., the spectrum occupancy pattern that would be perceived by a DSA/CR node) at longer time scales. Spectrum models for both cases are discussed in the following subsections.

2.2.1. Low time-resolution models

When the state of a primary radio channel is observed at low time-resolutions (i.e., the time period between consecutive channel observations is longer than the time period between consecutive changes in the channel state), the generalised Pareto distribution [17] constitutes an appropriate model for the perceived lengths of busy and idle periods, which is true in general regardless of the considered primary radio technology. Although other alternative distribution models may be able to provide comparable goodness-of-fits to empirical spectrum data in some particular cases, the generalised Pareto distribution provides, in average, the best overall fit over a wide range of spectrum bands and radio channels, for both busy and idle periods. The possibility to employ a single distribution model to characterise the lengths of busy and idle periods irrespective of the considered band and radio technology makes the generalised Pareto distribution an attractive alternative.

The cumulative distribution function (CDF) for the generalised Pareto distribution is given by:

$$F_{GP}(T;\mu,\lambda,\alpha) = 1 - \left[1 + \frac{\alpha(T-\mu)}{\lambda}\right]^{-1/\alpha} \tag{1.19}$$

where T represents the period length and μ, λ, α are the location, scale and shape parameters, respectively. The distribution parameters satisfy the following conditions:

$$T \geq \mu, \text{ for } \alpha \geq 0 \tag{1.20}$$

$$T \in \left[\mu, \mu - \frac{\lambda}{\alpha}\right] \text{for } \alpha < 0 \tag{1.21}$$

$$\mu > 0,\ \lambda > 0,\ \alpha < 1/2 \tag{1.22}$$

An arbitrary mean DC value can be obtained by selecting the parameters of the distribution in such a way that the following equality holds [4]:

$$\bar{\Psi} = \frac{\mathbb{E}\{T_1\}}{\mathbb{E}\{T_0\} + \mathbb{E}\{T_1\}} \tag{1.23}$$

where $\mathbb{E}\{T_0\}$ and $\mathbb{E}\{T_1\}$ represent the mean duration of idle and busy periods, respectively, which for the generalised Pareto distribution are given by:

$$\mathbb{E}\{T_i\} = \mu_i + \frac{\lambda_i}{1-\alpha_i},\ i \in \{0,1\} \tag{1.24}$$

The location parameter μ_i represents the minimum value of the observed period lengths T_i. Thus, in a DSA/CR system design, theoretical analysis or simulation tool, this parameter should be tailored to the particular scenario in accordance with the considered spectrum sensing for both T_0 and T_1.

2.2.2. High time-resolution models

When the state of a primary radio channel is observed at high time-resolutions (i.e., the time period between consecutive channel observations is notably shorter than the time period between consecutive changes in the channel state), the probability distribution that better fits the perceived lengths of busy and idle periods is highly dependent not only on the considered radio technology but also on the period type (idle or busy) as well. As an example, Table 1 shows some distributions that can be used to characterise the length of idle and busy periods in some wireless communication systems. Table 2 shows the corresponding mathematical expressions and distribution parameters.

Table 1 Probability distributions for high time-resolution models: Pareto (P), generalised Pareto (GP), generalised exponential (GE), gamma (G) and Weibull (W).

Primary radio technology/band	Idle periods	Busy periods
Amateur	GP, W, GE, G	GP
Paging	P	W, GE, G
TETRA	W or GP, P	GP, P or W
GSM/DCS	GE, G	GP

Table 2 Mathematical expressions and parameters of the probability distributions for high time-resolution models: Pareto (P), generalised exponential (GE), gamma (G) and Weibull (W). $\psi(\cdot)$ is the digamma function, $\gamma(\cdot,\cdot)$ is the lower incomplete gamma function and $\Gamma(\cdot)$ is the (complete) gamma function.

Distribution function	Parameters	$\mathbb{E}\{T_i\}$
$F_P(T;\lambda,\alpha)=1-\left(\frac{\lambda}{T}\right)^{\alpha}$	$T\geq\lambda$ $\lambda>0$ $\alpha>2$	$\frac{\alpha_i\lambda_i}{\alpha_i-1}$
$F_{GE}(T;\mu,\lambda,\alpha)=\left[1-e^{-\lambda(T-\mu)}\right]^{\alpha}$	$T\geq\mu>0$ $\lambda>0$ $\alpha>0$	$\mu_i+\frac{\psi(\alpha_i+1)-\psi(1)}{\lambda_i}$
$F_G(T;\mu,\lambda,\alpha)=\frac{\gamma\left(\alpha,\frac{T-\mu}{\lambda}\right)}{\Gamma(\alpha)}$	$T\geq\mu>0$ $\lambda>0$ $\alpha>0$	$\mu_i+\lambda_i\alpha_i$
$F_W(T;\mu,\lambda,\alpha)=1-\exp\left[-\left(\frac{T-\mu}{\lambda}\right)^{\alpha}\right]$	$T\geq\mu>0$ $\lambda>0$ $\alpha>0$	$\mu_i+\lambda_i\Gamma\left(1+\frac{1}{\alpha_i}\right)$

For any distribution, an arbitrary mean DC value can be obtained by selecting the parameters of the distributions in such a way that equation (1.23) is met, taking into account the expressions provided in Table 2 for $\mathbb{E}\{T_i\}$. The minimum value of the observed period lengths T_i (λ for the Pareto distribution and μ for the rest of distributions in Table 2) should be tailored to the particular scenario according to the minimum channel occupancy period, which in the particular case of time-slotted systems corresponds to the time-slot duration. For time-slotted systems, the lengths of busy and idle periods can alternatively be modelled from a discrete-time perspective, where the period lengths are described in terms of the number of time-slots. For example, for GSM/DCS systems, empirical data indicate that the number of 577-μs time-slots within a busy or idle period can be modelled as random variable with a negative binomial distribution. However, the continuous-time distributions provided in Table 1 and Table 2 constitute adequate modelling alternatives for time-slotted systems as well.

2.2.3. Combined low/high time-resolution models

The probability distribution models discussed in Sections 2.2.1 and 2.2.2 can be employed to characterise the spectrum occupancy pattern perceived by a DSA/CR user at long and short time scales, respectively. In both cases, the sequence of channel states can be described by a two-state CTSMC model where the idle and busy state holding times are described by two distribution functions $F(T_0)$ and $F(T_1)$ respectively. This section explores two different extensions to this simple modelling approach to simultaneously reproduce the statistical properties of spectrum usage at long and short time scales.

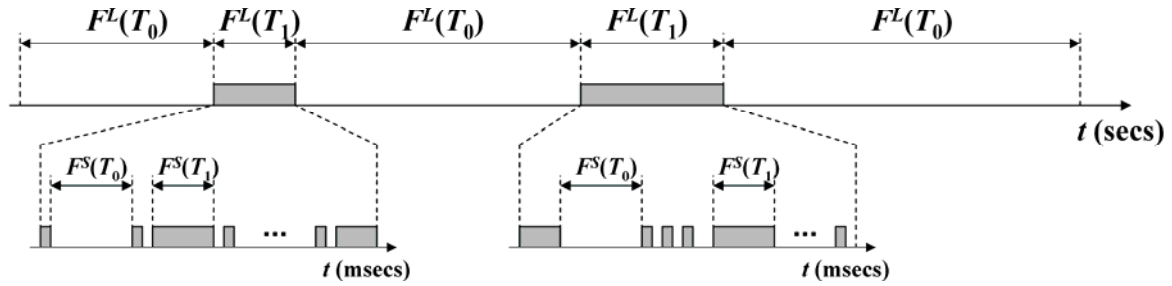

(a)

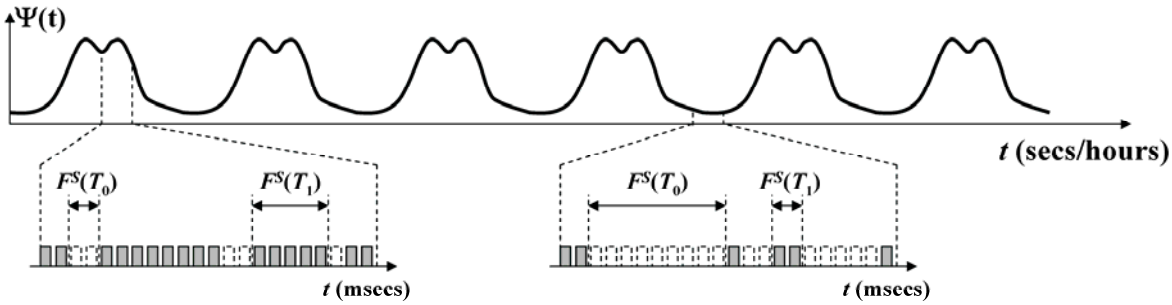

(b)

Figure 13 Combined low/high time-resolution models: (a) general modelling approach, (b) modelling approach for cellular mobile communication systems such as GSM/DCS.

The first approach comprises four distribution functions, two of them are used to describe the channel usage pattern in terms of the lengths of inactivity and activity periods at long time scales (e.g., seconds or minutes), $F^L(T_0)$ and $F^L(T_1)$ respectively, while the other two distributions describe the lengths of idle and busy periods at short time scales (e.g., microseconds or milliseconds), $F^S(T_0)$ and $F^S(T_1)$ respectively. According to this modelling approach, and as illustrated in Figure 13a, the distribution function $F^L(T_0)$ is used to model long inactivity periods, while the distribution function $F^L(T_1)$ is used to characterise the length of the periods over which some primary activity exists. During such activity periods, a sequence of idle and busy periods is present at a shorter time scale as described by the distribution functions $F^S(T_0)$ and $F^S(T_1)$. The functions $F^L(T_0)$ and $F^L(T_1)$ can be generalised Pareto distributions as discussed in Section 2.2.1, while $F^S(T_0)$ and $F^S(T_1)$ depend on the particular radio technology under study as discussed in Section 2.2.2 (the distributions provided in Table 1 and Table 2 can be used as a reference). This modelling approach is suitable for channels that remain inactive for relatively long periods of time until a primary transmitter becomes active, in which case a sequence of shorter busy/idle periods follows. Based on empirical observations for various radio technologies, this modelling approach is appropriate for channels of amateur bands, paging bands, private/public-access mobile radio (PMR/PAMR) bands and cordless telephone bands.

For channels of cellular mobile communication systems such as GSM 900 and DCS 1800, the existence of idle periods lasting for several seconds is rather unlikely. For this particular case, the modelling approach illustrated in Figure 13b is more convenient. This alternative considers two distribution functions to describe the length of idle and busy periods at short time scales, $F^S(T_0)$ and $F^S(T_1)$ respectively. The behaviour at long time scales is included by means of a DC model that

characterises the channel load variation over time. The DC models described in Sections 2.1.2.1 and 2.1.2.2 for cellular mobile communication systems can be employed to this end. Based on this approach, the parameters of the distribution functions $F^S(T_0)$ and $F^S(T_1)$ are regularly adjusted based on equation (1.23) so as to meet the corresponding DC, $\Psi(t)$, at any time. This alternative modelling approach is more appropriate in the case of GSM/DCS systems, where at least a few slots are frequently busy with a periodicity that depends on the load supported by the channel (i.e., the higher the load, the shorter the idle periods and the longer the busy periods and vice versa).

2.3. Time-correlation models

The DTMC and CTSMC modelling approaches described in Sections 2.1 and 2.2 are able to explicitly capture and reproduce the statistical distributions of busy and idle periods as well as the mean channel occupancy level, which is also implicitly included since it depends on the mean value of the distributions as indicated by equation (1.23). In some cases, however, the lengths of busy and idle periods can be correlated [16], a feature that the described modelling approaches cannot reproduce. This section explores the time-correlation properties of spectrum usage in real systems and presents adequate correlation models as well as a simulation method featuring correlated busy/idle periods [18].

2.3.1. Correlation metrics

The correlation properties of busy/idle periods can be quantified by means of the Pearson's product-moment correlation coefficient ρ, the Kendall's rank correlation coefficient τ, and the Spearman's rank correlation coefficient ρ_s [19]. All of them take values within the interval $[-1,\ +1]$. When the two considered random variables increase or decrease together, the correlation coefficients are positive. However, if one variable increases as the other decreases, then the correlation coefficients are negative. If the variables are independent, the correlation coefficients are zero (or approximately zero), but the converse is not true in general. There are, however, some important differences. First, ρ is only sensitive to linear dependence relations between random variables. Thus, if the association between two random variables is purely non-linear, then $\rho = 0$ even though they are not independent. On the other hand, τ and ρ_s can detect some non-linear associations between variables. Moreover, ρ has the unfortunate property of being sensitive (i.e., variant) under non-linear transformations of the random variables. However, τ and ρ_s are invariant under monotone transformations. Thus, given two random variables with correlation coefficients ρ, τ and ρ_s, a transformation of the variables could (and usually does) change the value of ρ, but it will not affect the values of τ and ρ_s under strictly monotone transformations.

2.3.2. Correlation properties of spectrum usage and models

The durations of consecutive busy-idle periods frequently show non-zero correlations in real systems, meaning that they are not independent in practice and, as such, need to be modelled as correlated random variables. The correlation between a busy period and the following idle period normally takes negative values, which can be explained by the fact that when the channel load increases the length of a busy period increases and the length of the next idle period tends to decrease and vice versa. Typical empirical values are comprised within the interval $[-0.6, 0)$ for the three correlation metrics discussed in Section 2.3.1, without important differences among them.

An additional correlation parameter is the correlation between the sequence of periods of the same type (either busy or idle) of a channel and a shifted version of itself, as a function of the shifting distance or lag number (i.e., the autocorrelation function of busy or idle periods). Two different autocorrelation patterns can be identified, namely a periodic pattern and a non-periodic pattern. As an

example, Figure 14 shows the autocorrelation function of idle periods as a function of the lag number, *m*, based on the Spearman's correlation coefficient, i.e., $\rho_s(T_0, T_0; m)$. Similar trends are observed for busy periods and the rest of correlation metrics.

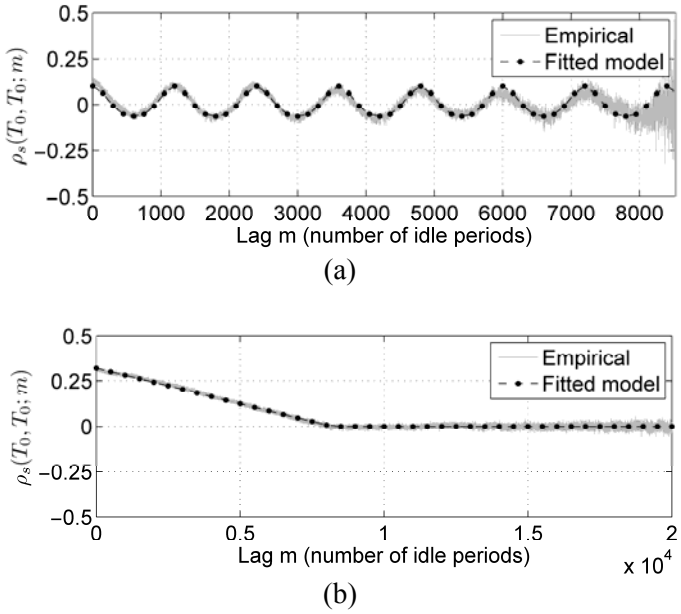

Figure 14 Autocorrelation function of busy or idle periods: (a) periodic pattern, (b) non-periodic pattern.

For channels with periodic autocorrelation functions (Figure 14a) with period M, the correlation coefficient can be expressed as the summation of two bell-shaped exponential terms centred at lags $m = 1$ and $m = M + 1$, with amplitudes A and widths σ:

$$\rho_s(T_i, T_i; m) = \begin{cases} 1, & m = 0 \\ \rho_s^{min} + Ae^{-\left(\frac{m-1}{\sigma}\right)^2} + Ae^{-\left(\frac{m-M-1}{\sigma}\right)^2}, & 1 \le m \le M \end{cases} \tag{1.25}$$

where ρ_s^{min} is the minimum correlation. This behaviour is commonly observed in cellular mobile communication systems where the experienced loads, and thus the busy/period lengths, show a relatively similar and periodic daily behaviour. Typical values for the parameters are $\rho_s^{min} \approx -0.1$, $A \in [0.2, 0.5]$, M is equal to the average number of lags equivalent to 24 hours, and $\sigma \approx M / 4$.

For channels with non-periodic autocorrelation functions (Figure 14b), the correlation coefficient takes its maximum value ρ_s^{max} at $m = 1$ and decreases linearly with m until $m = M$, beyond which the correlation is approximately zero. This behaviour can adequately be modelled by:

$$\rho_s(T_i, T_i; m) = \begin{cases} 1, & m = 0 \\ \rho_s^{max}\left(\frac{M - m}{M - 1}\right), & 1 \le m \le M \\ 0, & m > M \end{cases}$$

Typical values for the parameters are $\rho_s^{max} \in [0.1, 0.8]$ and $M \in [200, 10000]$.

2.3.3. Simulation of correlation properties

This section presents a simulation method to reproduce the time-correlation properties of spectrum usage observed in real systems. The method is based in some fundamental results and principles from the theory of random variate generation [19], which are reviewed in the following subsection.

2.3.3.1. Random variate generation principles

The inversion method

The inversion method [19] can be used to generate random variates with any arbitrary distribution. This method is based on the following property. Let $F(\cdot)$ be a continuous CDF on with inverse CDF given by $F^{-1}(\cdot)$. If U is a uniform random variable within the interval $[0,1]$, then the CDF of $F^{-1}(U)$ is $F(\cdot)$. Moreover, if X is a random variable with CDF $F(\cdot)$, then $F(X)$ is uniformly distributed on $[0,1]$. Based on this property, any distribution $F(\cdot)$ can be generated based on random variates with uniform or any other distributions.

Generation of correlated random variates

If Y and Z are independent and identically distributed (iid) random variables and a new random variable X is defined as:

$$X = \rho_0 Y + \sqrt{1-\rho_0^2}\, Z \tag{1.26}$$

with $\rho_0 \in [-1,+1]$, then X and Y have a Pearson's correlation coefficient $\rho(X,Y) = \rho_0$ [19]. This property can be used to generate random variates with a specified Pearson's correlation coefficient.

It is worth noting that the normal distribution is one of the few distributions that is stable, meaning that a linear combination of two independent variables of such distribution also has the same distribution, up to the location and scale parameters. Therefore, if Y and Z are normally distributed, then X is also normally distributed. Moreover, if Y and Z are standard (zero-mean, unit-variance) normal random variables, then X is also a standard normal random variable.

A sequence $X = x_1, x_2, \ldots, x_M$ of M standard normal random values with specified Pearson's autocorrelation function $\rho(X, X; m)$ can be generated based on the property:

$$F\{\rho(X, X; m)\} = \left|F\{X\}\right|^2 \tag{1.27}$$

derived from the Wiener-Khinchin theorem, where $F\{\cdot\}$ denotes the Fourier transform. Subjecting a standard Gaussian process to a linear operation (including filtering) yields another standard Gaussian process with a different autocorrelation function. Thus, an appropriate filter, derived from equation (1.27), can be used to induce correlation on an uncorrelated Gaussian process. Concretely, if $Y = y_1, y_2, \ldots, y_M$ is a sequence of iid complex standard normal random values, then [20]:

$$X = \mathrm{Re}\left\{F^{-1}\left\{Y \square \sqrt{|F\{\rho(X, X; m)\}|}\right\}\right\} \tag{1.28}$$

is a sequence $X = x_1, x_2, \ldots, x_M$ of standard normal random values with Pearson's autocorrelation function $\rho(X, X; m)$, where stands for Hadamard's element-wise multiplication.

Relation among correlation metrics

For normally distributed random variables X and Y, the correlation metrics considered in Section 2.3.1 are related as [21]:

$$\rho(X,Y) = \sin\left(\frac{\pi}{2}\tau(X,Y)\right) = 2\sin\left(\frac{\pi}{6}\rho_s(X,Y)\right) \tag{1.29}$$

Equation (1.29) holds if X and Y are normally distributed. If a monotone transformation is applied to X and/or Y, $\tau(X,Y)$ and $\rho_s(X,Y)$ will remain unchanged but $\rho(X,Y)$ might not.

2.3.3.2. Simulation method

Algorithm 1 shows a simulation method, based on the principles reviewed in Section 2.3.3.1, that reproduces any arbitrary distribution of busy/idle period lengths along with the correlation properties of spectrum usage discussed in Section 2.3.2. The algorithm requires as input information the CDF of idle and busy periods, denoted as $F_0(\cdot)$ and $F_1(\cdot)$ respectively, the Kendall or Spearman correlation coefficient between busy/idle periods, denoted as $\tau(T_0,T_1)$ and $\rho_s(T_0,T_1)$ respectively, as well as the autocorrelation function (periodic or non-periodic) of idle periods in terms of the Kendall or Spearman correlation coefficients as a function of the lag number m, i.e., $\tau(T_0,T_0;m)$ or $\rho_s(T_0,T_0;m)$ respectively. Notice that the desired correlations to be reproduced need to be specified in terms of the Kendall or Spearman metrics since the algorithm involves some transformations of random variables that would change any specified Pearson's correlation value. The same algorithm can be used to reproduce the autocorrelation properties of busy periods, i.e., $\tau(T_1,T_1;m)$ or $\rho_s(T_1,T_1;m)$, instead of idle periods, if desired. However, idle periods represent the real spectrum opportunities for secondary users and modelling their autocorrelation properties results therefore more convenient. The proposed algorithm outputs sequences of period durations for idle periods (T_0) and busy periods (T_1) in blocks of M values.

For periodic idle autocorrelation functions, M corresponds to the function's period and determines the periodicity with which the process is repeated. For non-periodic idle autocorrelation functions, M represents the lag number beyond which autocorrelation is negligible. In such a case, after generating a sequence of M period lengths, a new one is generated based on different (independent) random variates.

First of all, the correlation properties specified in terms of the Kendall or Spearman metrics are converted to their Pearson counterpart based on equation (1.29) (lines 1 and 2). Afterwards, and for every block of M values, a sequence ϑ of M iid complex standard normal variates is generated (line 4) and converted, based on equation (1.28), into a sequence ξ_0 (line 5) of standard normal variates with autocorrelation function $\rho(T_0,T_0;m)$. A sequence χ of M iid standard normal variates is generated (line 6) in order to produce, based on equation (1.26), a sequence ξ_1 (line 7) that has a correlation $\rho(T_0,T_1)$ with ξ_0. Since ξ_0 and ξ_1 are standard normal variates, the new random variables $\Phi(\xi_0)$ and $\Phi(\xi_1)$, where:

$$\Phi(x) = \frac{1}{2}\left[1 + \mathrm{erf}\left(\frac{x}{\sqrt{2}}\right)\right] \tag{1.30}$$

is the standard normal CDF, are uniformly distributed. Thus, by the inversion principle, the transformations of lines 8 and 9 produce sequences T_0 and T_1 of M period lengths with the desired CDFs. Moreover, since ξ_0 and ξ_1 are normally distributed, the desired Kendall and Spearman correlations hold between them as inferred from equation (1.29). Therefore, the monotone transformations of lines 8 and 9 preserve such correlations on T_0 and T_1. As a result, this procedure yields a sequence of idle and busy periods, T_0 and T_1 respectively, that follow the specified distributions $F_0(\cdot)$ and $F_1(\cdot)$, where idle periods are characterised by an autocorrelation function $\tau(T_0,T_0;m)$ or $\rho_s(T_0,T_0;m)$ and the correlation between busy-idle periods is given by $\tau(T_0,T_1)$ or $\rho_s(T_0,T_1)$.

Algorithm 1 Simulation of time correlation properties

Input: $F_0(\cdot)$, $F_1(\cdot)$, $\tau(T_0,T_1)$ or $\rho_s(T_0,T_1)$, $\tau(T_0,T_0;m)$ or $\rho_s(T_0,T_0;m)$

Output: T_0, T_1

1: $\rho(T_0,T_1) \leftarrow f\left(\{\tau(T_0,T_1)|\rho_s(T_0,T_1)\}\right)$

2: $\rho(T_0,T_0;m) \leftarrow f\left(\{\tau(T_0,T_0;m)|\rho_s(T_0,T_0;m)\}\right)$

3: **for** every block of M values **do**

4: Generate $\vartheta = \vartheta_1, \vartheta_2, \ldots, \vartheta_M \sim CN(0,1)$

5: $\xi_0 \leftarrow \mathrm{Re}\{F^{-1}\{\vartheta \sqrt{|F\{\rho(T_0,T_0;m)\}|}\}\}$

6: Generate $\chi = \chi_1, \chi_2, \ldots, \chi_M \sim N(0,1)$

7: $\xi_1 \leftarrow \rho(T_0,T_1)\cdot\xi_0 + \sqrt{1-[\rho(T_0,T_1)]^2}\cdot\chi$

8: $T_0 \leftarrow F_0^{-1}\left(\Phi\left(\xi_0\right)\right)$

9: $T_1 \leftarrow F_1^{-1}\left(\Phi\left(\xi_1\right)\right)$

10: **end for**

3. Time-frequency models

This section extends the models presented in Section 2 by introducing the frequency dimension of spectrum usage. The models discussed in this section can be employed to capture and reproduce the time evolution of the occupancy patterns observed in a group of channels belonging to the same allocated spectrum band. The joint behaviour of the set of channels within the same spectrum band is a statistical characteristic that needs to be accurately modelled since it has a direct impact on the amount of consecutive vacant spectrum that a DSA/CR user may find as well as the time period for which spectrum holes can be exploited for opportunistic use. Furthermore, a sophisticated procedure to generate artificial spectrum occupancy data for simulation or other purposes is described as well. The presented method is capable to accurately capture and reproduce the statistical time-frequency characteristics of spectrum usage in real systems.

3.1. Joint time-frequency properties of spectrum usage

An important aspect of joint spectrum occupancy modelling in the time and frequency dimensions is the potential existence of dependence relations between the occupancy patterns observed in both dimensions. In other words, it is important to determine whether the binary time-occupancy pattern of a radio channel depends on other channels within the same band or, on the contrary, the individual channel occupancy patterns are mutually independent. The analysis of empirical data [22] indicates

that the occupancy patterns for channels within a spectrum band can be considered to be mutually independent. This is a result with important implications for joint time-frequency modelling, since it implies that the instantaneous occupancy state of a channel is unrelated to the instantaneous state of the rest of channels within the considered band and, consequently, the occupancy patterns of a group of channels can be modelled independently of each other. On the one hand, this enables the direct application of the time-domain models developed in Section 2 without any modifications or additional considerations. On the other hand, this enables the statistical properties of spectrum usage over frequency to be analysed and modelled independently of the time-dimension statistics, which is performed in Section 3.2.

3.2. Frequency-dimension models

Two relevant properties of spectrum usage in the frequency dimension deserve explicit consideration in frequency-domain models. The first property is the probability distribution of the DC values for channels within the same band. The second property is the DC clustering over frequency, i.e., the existence of groups of contiguous channels with similar DC values. Both aspects are discussed in detail in the following subsections.

3.2.1. Duty cycle distribution models

Assuming that the DSA/CR system operates over a set of C primary radio channels, denoted by $\Upsilon = \{\upsilon_1, \upsilon_2, \ldots, \upsilon_c, \ldots, \upsilon_C\}$, and given the set $\boldsymbol{\Psi} = \{\Psi_1, \Psi_2, \ldots, \Psi_c, \ldots, \Psi_C\}$, where Ψ_c is the DC of channel υ_c, the probability distribution of the elements of $\boldsymbol{\Psi}$ can accurately be fitted with the beta [9] and Kumaraswamy [10] distributions. The CDF for the former is given by:

$$F_B(x;\alpha,\beta) = I_x(\alpha,\beta) = \frac{B_x(\alpha,\beta)}{B(\alpha,\beta)}, \quad x \in (0,1) \tag{1.31}$$

where $\alpha > 0$ and $\beta > 0$ are shape parameters, $I_x(\alpha,\beta)$ is the regularised incomplete beta function, $B_x(\alpha,\beta)$ is the incomplete beta function given by:

$$B_x(\alpha,\beta) = \int_0^x z^{\alpha-1}(1-z)^{\beta-1}dz \tag{1.32}$$

and $B(\alpha,\beta)$ is the beta function given by equation (1.16). The CDF for the latter is given by:

$$F_K(x;a,b) = 1-\left(1-x^a\right)^b, \quad x \in (0,1) \tag{1.33}$$

where $a > 0$ and $b > 0$ are shape parameters.

Figure 15 shows some examples of empirical DC distributions and their corresponding beta and Kumaraswamy fits. The selected bands represent examples for a wide variety of load levels, including very low (E-GSM 900 UL), low (DECT), medium (ISM) and very high (E-GSM 900 DL) average band DCs. The models can be configured in order to reproduce any arbitrary average DC over the whole band by selecting the shape parameters according to equation (1.18).

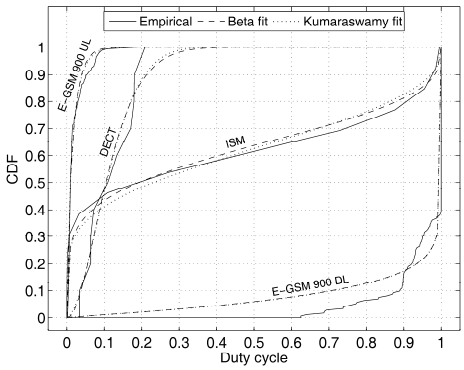

Figure 15 Empirical DC distributions and their corresponding beta and Kumaraswamy fits.

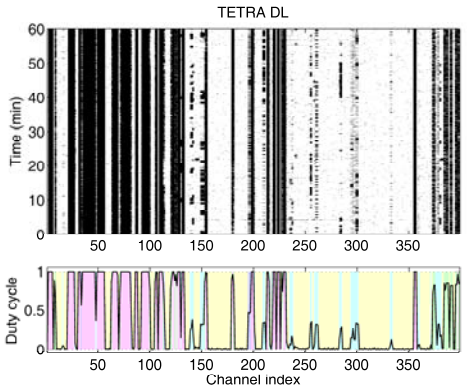

Figure 16 Example of empirical DC clustering (TETRA downlink band).

3.2.2. Duty cycle clustering models

Channels with similar load/DC levels rarely occur alone, but in groups of a certain size. The existence of groups of contiguous channels with similar DC values can be analysed and modelled by defining a set of DC archetypes. As a reference, the following DC archetypes can be considered: very low $\Psi \in [0, 0.05]$, low $\Psi \in (0.05, 0.40]$, medium $\Psi \in (0.40, 0.60]$, high $\Psi \in (0.60, 0.95]$ and very high $\Psi \in (0.95, 1]$ levels. Based on these archetypes, Figure 16 shows an example of DC clustering in the TETRA downlink band (the upper graph shows the instantaneous spectrum occupancy for each channel for a time period of 60 minutes, where white/black points indicate idle/busy observations respectively, while the lower graph shows the channel DCs and their corresponding classification into the considered archetypes). As it can clearly be appreciated, channels with similar occupancy levels appear together in blocks of a certain size, i.e. the DC is clustered in the frequency domain. The number of contiguous channels per cluster (i.e., group of channels belonging to the same DC archetype) can be modelled as a geometrically distributed random variable, whose CDF is given by [9]:

$$F_{Geom}(k; p) = 1 - (1 - p)^k, \quad k \in \mathbb{N}^* = \{1, 2, 3, \ldots\}$$

where k represents the number of channels belonging to the same group (i.e., the cluster size) and $1/p$ ($0 \le p \le 1$) represents its expected (mean) value, i.e. $\mathbb{E}\{k\} = 1/p$. The value of the parameter p can be set for a particular average number M of channels per cluster as $p = 1/M$. The relation $p \approx C \cdot 10^{-3}$, with C being the number of channels in the whole band, can be used as an empirical approximation as long as the resulting value satisfies $p \le 1$. An alternative empirical approximation is to draw the value of p from a uniform distribution within the interval $[0.1,\ 0.6]$.

3.3. Simulation method

This section presents a procedure that can be employed to generate artificial time-frequency spectrum data in simulation tools or for other purposes. The method is composed of three phases.

Phase 1: Generation of DC values.

Step 1.1: Specify the number C of channels within the considered spectrum band.

Step 1.2: Select a DC distribution function $F(\Psi)$ (beta or Kumaraswamy) and appropriate values for the distribution parameters.

Step 1.3: Based on the probability distribution resulting from Step 1.2, generate a set of C independent random numbers, which will constitute the set $\underline{\boldsymbol{\Psi}} = \{\hat{\Psi}_1, \hat{\Psi}_2, \ldots, \hat{\Psi}_c, \ldots, \hat{\Psi}_C\}$ of DC values to be assigned to the C channels of the considered spectrum band.

Phase 2: Assignment of DC values to channels.

Step 2.1: Define a set $A = \{A_1, A_2, \ldots, A_n, \ldots, A_N\}$ of N DC archetypes along with the corresponding set $\boldsymbol{\Lambda} = \{\Lambda_0, \Lambda_1, \ldots, \Lambda_n, \ldots, \Lambda_N\}$ of $N+1$ DC thresholds, where $\Lambda_0 = 0$ and $\Lambda_N = 1$. A DC $\hat{\Psi}_c$ belongs to archetype A_n if $\Lambda_{n-1} < \hat{\Psi}_c \leq \Lambda_n$.

Step 2.2: Based on the probability distribution resulting from Step 1.2, compute the elements of the set $\boldsymbol{\Pi} = \{\Pi_1, \Pi_2, \ldots, \Pi_n, \ldots, \Pi_N\}$, where $\Pi_n = P(A_n) = P(\Lambda_{n-1} < \hat{\Psi}_c \leq \Lambda_n) = F(\Lambda_n) - F(\Lambda_{n-1})$ represents the probability that a channel belongs to archetype A_n.

Step 2.3: Classify the values of set $\underline{\boldsymbol{\Psi}}$ into the archetypes of set A based on the threshold set $\boldsymbol{\Lambda}$. This produces N subsets $\{\underline{\boldsymbol{\Psi}}_n\}_{n=1,\ldots,N}$ (one per DC archetype) with $\eta_n = |\underline{\boldsymbol{\Psi}}_n|$ elements each satisfying the conditions $\bigcup_{n=1}^{N} \underline{\boldsymbol{\Psi}}_n = \underline{\boldsymbol{\Psi}}$ and $\bigcap_{n=1}^{N} \underline{\boldsymbol{\Psi}}_n = \varnothing$.

Step 2.4: Select an appropriate value for the parameter p of the geometric distribution of the number of channels per cluster.

Step 2.5: Set to zero the elements of $\boldsymbol{\Psi} = \{\Psi_1, \Psi_2, \ldots, \Psi_c, \ldots, \Psi_C\}$, where Ψ_c represents the DC value finally assigned to channel υ_c. Set to zero the elements of the set $\boldsymbol{\alpha} = \{\alpha_1, \alpha_2, \ldots, \alpha_n, \ldots, \alpha_N\}$, where α_n represents a counter of the number of channels belonging to DC archetype A_n with an assigned final DC value. Define the counter $\alpha_C = \sum_{n=1}^{N} \alpha_n$ for the overall number of channels with an already assigned DC value. Repeat the following points until $\alpha_n = \eta_n$ for all n (i.e., $\alpha_C = \sum_{n=1}^{N} \eta_n = C$):

1. Decide the DC archetype $A' = A_n$ for the next cluster (i.e., the next group of channels) by generating a uniformly distributed $U(0,1)$ random variate and comparing against the probabilities of the set $\boldsymbol{\Pi}$.

2. If this is not the first iteration of the process and the archetype A' resulting from point 1 is of the same type as the archetype A'' of the previously generated cluster, or

if the number of channels for archetype $A'=A_n$ has already been reached ($\alpha_n = \eta_n$), go back to point 1 and recompute A' until the conditions $A' \neq A''$ and $\alpha_n < \eta_n$ are met. The condition $A' \neq A''$ is not necessary when there is a single DC archetype for which $\alpha_n < \eta_n$.

3. Decide the number χ of channels that belong to the new cluster of type $A'=A_n$ as a random number drawn from the geometric distribution obtained in Step 2.4. If $\alpha_n + \chi > \eta_n$, then perform the correction $\chi = \eta_n - \alpha_n$ in order to meet the total number of channels per archetype.

4. Select randomly χ DC values from subset $\boldsymbol{\Psi}_n$ (archetype A_n) that have not been assigned yet in order to form the subset $\hat{\boldsymbol{\Psi}} = \{\hat{\Psi}_1, \hat{\Psi}_2, \ldots, \hat{\Psi}_\chi\} \subseteq \boldsymbol{\Psi}_n$. Append subset $\hat{\boldsymbol{\Psi}}$ to the set of DC values already assigned, i.e., $\{\Psi_{\alpha_C+1}, \Psi_{\alpha_C+2}, \ldots, \Psi_{\alpha_C+\chi}\} = \{\hat{\Psi}_1, \hat{\Psi}_2, \ldots, \hat{\Psi}_\chi\} = \hat{\boldsymbol{\Psi}}$.

5. Update counters $\alpha_n = \alpha_n + \chi$ and $\alpha_C = \alpha_C + \chi$. Go to point 1.

Phase 3: Generation of time-domain occupancy sequences.

Step 3.1: Select appropriate distributions $F_0(T_0)$ and $F_1(T_1)$ for the length T_0 of idle periods and the length T_1 of busy periods, respectively.

Step 3.2: Configure the parameters of the distributions selected in Step 3.1 in such a way that the channels' average DCs meet the DC values obtained in Step 2.5, i.e. $\mathbb{E}\{T_1^c\} / (\mathbb{E}\{T_0^c\} + \mathbb{E}\{T_1^c\}) = \Psi_c$, where $\mathbb{E}\{T_0^c\}$ and $\mathbb{E}\{T_1^c\}$ are the mean length of idle and busy periods, respectively, for the *c*-th channel, υ_c.

Step 3.3: Generate for every channel a sequence of consecutive idle/busy periods whose lengths are drawn from the properly configured distributions $F_0(T_0)$ and $F_1(T_1)$. The sequences generated for every channel must be independent from each other. It is worth noting that the more sophisticated simulation method proposed in Section 2.3.3.2 can be used here in order to reproduce not only the distributions $F_0(T_0)$ and $F_1(T_1)$ but also correlation properties.

The steps conducted in the first phase guarantee that the DC values of the band follow an appropriate beta or Kumaraswamy distribution and consequently reproduce the corresponding average band DC. The second phase ensures that the DCs of contiguous channels respect the corresponding properties of DC clustering. Finally, the third phase provides the lengths of busy and idle periods for each channel so that not only the desired period length distributions are reproduced but also the appropriate DC distribution over frequency channels (and additionally the time-correlation properties of spectrum usage if the method of Section 2.3.3.2 is employed).

4. Space dimension models

The spatial models presented in this section are envisaged to describe the average level of occupancy (expressed in terms of the DC) that would be perceived by DSA/CR users at various geographical locations based on the knowledge of some simple primary signal parameters. Moreover, an extension is proposed in order to characterise not only the average occupancy perception but also the simultaneous observations of various DSA/CR users on the spectrum occupancy pattern of the same transmitter.

4.1. Models for average spectrum occupancy perception

The models presented in this section describe the spatial distribution of the DC [23]. The interest of employing the DC lies in its ability to summarise the overall spectrum occupancy within a certain time interval and frequency range in a single numerical value. The spatial distribution of the DC is employed by the models presented in this section as a means to describe the spectrum occupancy that would be perceived by secondary DSA/CR terminals at different geographical locations.

It is important to make a clear distinction between the Activity Factor (AF) of a primary transmitter in a certain channel and the DC perceived by secondary DSA/CR terminals in that channel. The AF of a primary transmitter represents the fraction of time that the transmitter is active (i.e., transmitting in the channel). A DSA/CR terminal in an arbitrary location with good radio propagation conditions with respect to the primary transmitter would observe the channel as busy whenever the primary transmitter is active. However, at other locations where the propagation conditions are not so favourable, the primary signal might not be detected. In such a case, the level of spectrum activity perceived by the DSA/CR terminal in terms of the DC would be lower than the actual AF of the primary transmitter. While the AF is unique for a given transmitter, the DC perceived at different locations may be different. Since the propagation conditions strongly vary with the geographical location, the perceived DC will vary over space accordingly. The models discussed in this section describe the spatial distribution of the DC as a function of the radio propagation conditions.

4.1.1. Received average power distribution

The occupancy state of a channel as perceived by a DSA/CR terminal depends on the employed spectrum sensing method [24]. Due to its simplicity, wide range of application and relevance, energy detection (ED) has been a preferred choice for DSA/CR. According to ED, a DSA/CR terminal measures the power received in a certain frequency band over a predefined time period T, which can be expressed as:

$$P_R = \frac{1}{T}\int_{-T/2}^{+T/2} P_R(t)dt \tag{1.34}$$

where $P_R(t)$ is the instantaneous power received by the DSA/CR terminal (including noise) and P_R is the average power over the sensing period T. The average power P_R is compared with a predefined threshold in order to decide on the primary channel state: if P_R is above the threshold the channel is declared to be busy; otherwise, it is assumed to be idle. The perceived spectrum occupancy at a particular location therefore depends on the statistics of the received average power, P_R. Note that the instantaneous power $P_R(t)$ is a stochastic process that can be thought of as a non-countable infinity of iid random variables, one for each time instant. Since P_R is obtained as the average of an infinite number of random variables, the central limit theorem can therefore be employed to approximate the PDF of P_R as a normal distribution, regardless of the real distribution of $P_R(t)$ [23].

4.1.2. Spatial duty cycle models

This section presents a set of models to describe and predict the spectrum occupancy perceived at various locations in terms of the DC. The DC can be defined as the probability that the channel is observed as busy. Note that the ED method will report the channel as busy whenever the average power P_R is above a certain decision threshold λ. Since ED is not able to distinguish between intended signals and undesired noise, the channel will be reported as busy not only if a primary signal is received above the decision threshold but also if there is no signal (or it is received below the threshold) and the noise power exceeds the threshold.

Let's denote the distribution of the noise power as $f_N(P_N) \sim N(\mu_N, \sigma_N^2)$ and the distribution of the signal power (received in the presence of noise) as $f_S(P_S) \sim N(\mu_S, \sigma_S^2)$. According to this formulation, μ_N represents the noise floor of the DSA/CR receiver and σ_N denotes the standard deviation of the noise powers P_N experienced at various sensing events (the effective noise power may be different between sensing events due to the finite averaging period T or other reasons such as temperature variations). The primary power P_S received in the presence of noise is characterised by an average value μ_S that depends on the transmission power and radio propagation conditions and a standard deviation σ_S that is additionally affected by the noise of the DSA/CR receiver.

If the sensed channel is idle, the PDF of the observed average power, $f_R(P_R)$, will be that of the noise, $f_N(P_N)$. In such a case, the probability that the observed power is above the threshold (i.e., the perceived DC) is given by (see Figure 17):

$$\Psi_{idle} = \int_{\lambda}^{\infty} f_R(P_R) dP_R = \int_{\lambda}^{\infty} f_N(P_N) dP_N = P_{fa} \tag{1.35}$$

where it has been assumed that the decision threshold λ is set so as to meet a specified target probability of false alarm P_{fa}.

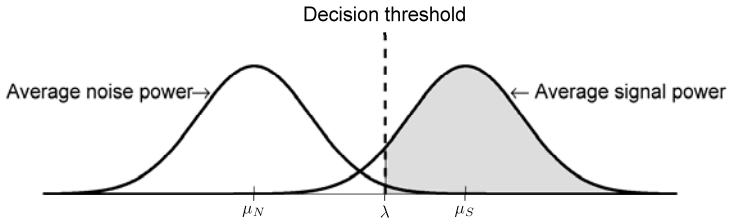

Figure 17 Model considered to compute the DC (shaded area).

On the other hand, if the channel is busy when it is sensed, the PDF of the observed average power, $f_R(P_R)$, will be that of the received signal, $f_S(P_S)$. Assuming an ideal situation where there is no noise, the DC perceived by the DSA/CR user would be given by:

$$\begin{aligned} \Psi_{busy}^{ideal} &= \int_{\lambda}^{\infty} f_R(P_R) dP_R = \int_{\lambda}^{\infty} f_S(P_S) dP_S \\ &= \frac{1}{\sqrt{2\pi}\sigma_S} \int_{\lambda}^{\infty} e^{-\frac{1}{2}\left(\frac{P_S - \mu_S}{\sigma_S}\right)^2} dP_S = Q\left(\frac{\lambda - \mu_S}{\sigma_S}\right) \end{aligned} \tag{1.36}$$

where $Q(\cdot)$ represents the Gaussian Q-function. Notice that equation (1.36) indicates that the perceived occupancy in terms of the DC would tend to zero as the received power decreases (i.e., $\mu_S \to -\infty$). However, if the received signal power is below the receiver's noise, this situation would be equivalent to an idle channel where the receiver observes only noise. In such a case, the perceived DC should be P_{fa} as indicated by equation (1.35). A more realistic model for $f_R(P_R)$ when the channel is busy, taking into account the presence of noise, would be $f_R(P_R) = M\left\{ f_N(P_N), f_S(P_S)\right\}$, where $M\{\cdot\}$ denotes a *realisation-wise maximum operator* defined as follows. If $A = \{x_{a_1}, x_{a_2}, \ldots, x_{a_n}, \ldots, x_{a_N}\}$ and $B = \{x_{b_1}, x_{b_2}, \ldots, x_{b_n}, \ldots, x_{b_N}\}$ represent two sets of N random numbers (realisations) drawn from distributions $f_a(x_a)$ and $f_b(x_b)$, respectively, then $f_c(x_c) = M\{f_a(x_a), f_b(x_b)\}$ represents the distribution of the elements of the set $C = \{x_{c_1}, x_{c_2}, \ldots, x_{c_n}, \ldots, x_{c_N}\}$, where $x_{c_n} = \max\{x_{a_n}, x_{b_n}\}$ for $n = 1, 2, \ldots, N$, when N tends towards infinity. Notice that this operator reproduces the effect of the noise floor on the observed power (i.e., the DSA/CR user observes the received signal power when it is above the noise floor or the noise power otherwise). Therefore, this definition of $f_R(P_R)$ provides a more realistic model for the average power P_R actually observed by the DSA/CR receiver. Based on this model, the DC perceived by the DSA/CR user when the channel is busy will then be given by:

$$\begin{aligned} \Psi_{busy}^{real} &= \int_{\lambda}^{\infty} f_R(P_R)dP_R = \int_{\lambda}^{\infty} M\left\{ f_N(P_N), f_S(P_S)\right\} dP_R \\ &= \max\left\{ \int_{\lambda}^{\infty} f_N(P_N)dP_N, \int_{\lambda}^{\infty} f_S(P_S)dP_S \right\} = \max\left\{ P_{fa}, Q\left(\frac{\lambda - \mu_S}{\sigma_S} \right) \right\} \end{aligned} \tag{1.37}$$

As it can be appreciated, this model rightly predicts that the perceived activity level is never lower than the target P_{fa}. The average DC perceived by the DSA/CR user will depend on the transmission power of the primary transmitter and its particular activity pattern. The next sections provide closed-form expressions for various general cases.

4.1.2.1. Constant-power continuous transmitters

This section considers the particular case of constant-power primary transmitters with an AF of 100% (e.g., TV and audio broadcasting services). This case provides the basis for a simple occupancy model that will be extended in the next sections for variable-power transmitters and/or discontinuous transmission patterns.

If the primary transmitter is always active, the PDF of the received average power $f_R(P_R)$ will be that of the primary signal (with noise) at the location of the DSA/CR terminal, i.e., $f_R(P_R) = M\left\{ f_N(P_N), f_S(P_S)\right\}$. The probability that the received average power P_R is above the decision threshold λ and the DSA/CR user observes the channel as busy is given by equation (1.37). Assuming that the decision threshold is set to meet a certain P_{fa}:

$$P_{fa} = \int_{\lambda}^{\infty} f_N(P_N)dP_N = \frac{1}{\sqrt{2\pi}\sigma_N} \int_{\lambda}^{\infty} e^{-\frac{1}{2}\left(\frac{P_N - \mu_N}{\sigma_N}\right)^2} dP_N = Q\left(\frac{\lambda - \mu_N}{\sigma_N} \right) \tag{1.38}$$

Solving in equation (1.38) for λ yields the decision threshold:

$$\lambda = Q^{-1}(P_{fa})\sigma_N + \mu_N \tag{1.39}$$

where $Q^{-1}(\cdot)$ denotes the inverse of $Q(\cdot)$. Substituting equation (1.39) into equation (1.37) finally yields the DC model:

$$\Psi = \max\left\{P_{fa}, Q\left(\frac{Q^{-1}(P_{fa})\sigma_N - \Gamma}{\sigma_S}\right)\right\} \tag{1.40}$$

where $\Gamma = \mu_S - \mu_N$ represents the average SNR expressed in decibels, while σ_S and σ_N are the standard deviation of the signal and noise average powers also in decibels.

4.1.2.2. Constant-power discontinuous transmitters

This section extends the model of equation (1.40) by including the case of constant-power but non-continuous transmitters. If the primary transmitter is characterised by a certain AF, denoted as $0 < \alpha < 1$, the PDF of the received average power $f_R(P_R)$ will be that of the primary signal (with noise) $M\{f_N(P_N), f_S(P_S)\}$ whenever the transmitter is active (which will occur with probability α) or noise $f_N(P_N)$ otherwise. Hence:

$$f_R(P_R) = (1-\alpha) f_N(P_N) + \alpha M\{f_N(P_N), f_S(P_S)\} \tag{1.41}$$

and the resulting expression for the DC becomes:

$$\begin{aligned}
\Psi &= \int_\lambda^\infty f_R(P_R) dP_R \\
&= (1-\alpha)\int_\lambda^\infty f_N(P_N) dP_N + \alpha \int_\lambda^\infty M\{f_N(P_N), f_S(P_S)\} dP_R \\
&= (1-\alpha)\int_\lambda^\infty f_N(P_N) dP_N + \alpha \max\left\{\int_\lambda^\infty f_N(P_N) dP_N, \int_\lambda^\infty f_S(P_S) dP_S\right\} \\
&= (1-\alpha) P_{fa} + \alpha \max\left\{P_{fa}, Q\left(\frac{Q^{-1}(P_{fa})\sigma_N - \Gamma}{\sigma_S}\right)\right\}
\end{aligned} \tag{1.42}$$

Notice that equation (1.40) is a particular case of equation (1.42) with $\alpha = 1$.

4.1.2.3. Variable-power discontinuous transmitters

This section extends the model to account for variable-power transmitters. In this case, the average transmission power is not constant but characterised by a certain PDF. To simplify the model, let's assume that the variability of the transmission power can adequately be described by a discrete set of K average transmission power levels, instead of a continuous PDF. This assumption not only simplifies the analytical expressions of the model, but also enables the application of the model to the case in which a channel is time-shared by K transmitters with different power levels as it may be the case of various TDMA-based systems such as GSM/DCS, TETRA, etc. The model can embrace the cases of a single variable-power transmitter with K transmission power levels and K constant-power transmitters time-sharing the channel. In both cases, the problem reduces to the possibility of observing K different average transmission powers in the channel.

Let's denote as $f_{S_k}(P_{S_k})$, with mean μ_{S_k} and standard deviation σ_{S_k}, the PDF of the received average power at certain location when the *k*-th transmission power level is present in the channel ($k = 1, 2, \ldots, K$). In general it can be assumed that $\mu_{S_p} \neq \mu_{S_q}$ and $\sigma_{S_p} \neq \sigma_{S_q}$ for $p \neq q$. Let's define an AF α_k for each transmission power representing the probability that the *k*-th transmission power level is present in the channel. In the case of a single-transmitter with K transmission power levels, only one out of the K power levels can be selected at a time. Moreover, in the case of K transmitters time-sharing the channel it is reasonable to assume that there exists some MAC mechanism so that when one primary transmitter accesses the channel the rest of potential primary transmitters remain inactive. In both cases, the K average power levels are mutually exclusive events. Hence:

$$\sum_{k=1}^{K} \alpha_k \leq 1 \tag{1.43}$$

where the equality holds when the channel is always busy.

The left-hand side of equation (1.43) represents the probability that any of the K transmitters is active, i.e. the probability that the channel is busy, and its complementary probability $1 - \sum_{k=1}^{K} \alpha_k$ is the probability that the channel is idle. The PDF of the received average power $f_R(P_R)$ will be that of the *k*-th primary signal (with noise) $M\left\{ f_N(P_N), f_{S_k}(P_{S_k}) \right\}$ whenever the *k*-th transmission power is active (which will occur with probability α_k) or it will be noise $f_N(P_N)$ otherwise. Hence:

$$f_R(P_R) = \left(1 - \sum_{k=1}^{K} \alpha_k \right) f_N(P_N) + \sum_{k=1}^{K} \alpha_k M\left\{ f_N(P_N), f_{S_k}(P_{S_k}) \right\} \tag{1.44}$$

and the resulting expression for the DC becomes:

$$\begin{aligned}
\Psi &= \int_{\lambda}^{\infty} f_R(P_R) dP_R \\
&= \left(1 - \sum_{k=1}^{K} \alpha_k \right) \int_{\lambda}^{\infty} f_N(P_N) dP_N + \sum_{k=1}^{K} \alpha_k \int_{\lambda}^{\infty} M\left\{ f_N(P_N), f_{S_k}(P_{S_k}) \right\} dP_R \\
&= \left(1 - \sum_{k=1}^{K} \alpha_k \right) \int_{\lambda}^{\infty} f_N(P_N) dP_N + \sum_{k=1}^{K} \alpha_k \max\left\{ \int_{\lambda}^{\infty} f_N(P_N) dP_N, \int_{\lambda}^{\infty} f_{S_k}(P_{S_k}) dP_{S_k} \right\} \\
&= \left(1 - \sum_{k=1}^{K} \alpha_k \right) P_{fa} + \sum_{k=1}^{K} \alpha_k \max\left\{ P_{fa}, Q\left(\frac{Q^{-1}(P_{fa})\sigma_N - \Gamma_k}{\sigma_{S_k}} \right) \right\}
\end{aligned}$$

where $\Gamma_k = \mu_{S_k} - \mu_N$ is the SNR resulting from the *k*-th average transmission power level expressed in decibels.

4.2. Models for concurrent snapshots observations

The models described in Section 4.1 can be employed to describe the average level of occupancy (expressed in terms of the DC) that would perceived by DSA/CR users at various geographical locations based on the knowledge of some simple primary signal parameters. In some cases it can be useful to characterise not only the average level of perceived spectrum occupancy but also the simultaneous observations of several DSA/CR users at various locations. This is the case, for instance, of cooperative techniques such as cooperative spectrum sensing where the nodes of a DSA/CR network exchange sensing information (e.g., the channel state observed by each DSA/CR terminal) in order to provide, based on an appropriate processing of the gathered information, a more reliable estimation on the actual busy/idle channel state. The gain of cooperative spectrum sensing and other cooperative techniques can be characterised and analysed in terms of simultaneous observations. For example, a group of DSA/CR nodes behind the same building would be affected by the same level of shadowing. In such a case, they would probably experience a similar average SNR and all of them might not detect the presence of a primary transmission. However, other DSA/CR nodes not affected by the same building and experiencing higher SNRs might be able to detect the presence of the licensed transmission and avoid situations of harmful interference. The characterisation of the simultaneous observations of various DSA/CR users as a function of their geographical locations or experienced SNRs is of great utility in this type of studies. The model developed in Section 4.1 is extended with some additional considerations to characterise the concurrent observations of various DSA/CR users at different locations.

The simultaneous observations at two different locations can be characterised in terms of the joint probability that the channel is observed at both locations in certain states or the conditional probability that it is observed in a certain state in one location given that it has been observed in a specified state at the other location. This probabilistic characterisation can be extended to any arbitrary number of locations by taking one location as a reference point and comparing to the rest of considered locations in pairs. This section analyses the joint and conditional probabilities between any two locations where one of them, the reference location, corresponds to the location where the primary signal is received at a SNR higher than that of any other location inside the geographical area under study (i.e., at the maximum experienced SNR).

The state space for a primary radio channel can be denoted as $\mathbb{S} = \{s_0, s_1\}$, where the s_0 state indicates that the channel is idle and the s_1 state indicates that the channel is busy. Let's denote as $P(s_i, s_j^*)$, with $i, j \in \{0,1\}$, the joint probability that the channel is simultaneously observed in state s_i at an arbitrary location and in state s_j at the reference location. Let's denote as $P(s_i|s_j^*)$ the conditional probability that the channel is observed in state s_i at an arbitrary location given that it has been observed in state s_j at the reference location. As previously mentioned, the SNR Γ^* at the reference location is greater than the SNR Γ at any other location ($\Gamma^* \geq \Gamma$), which implies that the DC Ψ^* perceived at that location satisfies the condition $\Psi^* \geq \Psi$ for all the Ψ values observed at all the other locations over the geographical area under study. This section derives the expressions of $P(s_i, s_j^*)$ and $P(s_i|s_j^*)$ for any arbitrary location as a function of the average DCs perceived at that location (Ψ) and the reference location (Ψ^*).

The set of conditional probabilities $P(s_i|s_j^*)$ can be derived as follows. When the channel is observed as idle at the reference location, this means that the channel is actually idle or the power received at the reference location is below the decision threshold. In the latter case, the power received at any location whose receiving SNR is lower will also be below the decision threshold and the channel will also be observed as idle. However, there exists a probability P_{fa} that the channel is observed as busy

because of noise samples above the threshold. Thus, $P(s_1|s_0^*) = P_{fa}$ and its complementary probability is $P(s_0|s_0^*) = 1 - P_{fa}$. On the other hand, when the channel is observed as busy at the reference location, this means that there has been a false alarm at the reference receiver or the channel is actually busy and it has been received at the reference location with a power level above the decision threshold. In this case, the probability that the channel is observed as busy/idle at an arbitrary location depends not only on the probability of false alarm but also the experienced SNR Γ and its relation to the reference SNR Γ^*. The conditional probability $P(s_0|s_1^*)$ can be derived by writing the probability $P(s_0)$ that the channel is observed as idle at the arbitrary location as:

$$\begin{aligned} P(s_0) &= P(s_0|s_0^*)P(s_0^*) + P(s_0|s_1^*)P(s_1^*) \\ &= (1 - P_{fa})(1 - \Psi^*) + P(s_0|s_1^*)\Psi^* = 1 - \Psi \end{aligned} \tag{1.45}$$

where $P(s_j^*)$ represents the probability that the channel is observed in state s_j at the reference location and it has been made use of the equivalence $P(s_0) = 1 - \Psi$. Solving equation (1.45) for the desired term yields:

$$P(s_0|s_1^*) = \frac{1 - \Psi - (1 - P_{fa})(1 - \Psi^*)}{\Psi^*} \tag{1.46}$$

Following a similar procedure:

$$\begin{aligned} P(s_1) &= P(s_1|s_0^*)P(s_0^*) + P(s_1|s_1^*)P(s_1^*) \\ &= P_{fa}(1 - \Psi^*) + P(s_1|s_1^*)\Psi^* = \Psi \end{aligned} \tag{1.47}$$

which yields:

$$P(s_1|s_1^*) = \frac{\Psi - P_{fa}(1 - \Psi^*)}{\Psi^*} \tag{1.48}$$

The set of joint probabilities can readily be obtained based on their conditional counterparts as $P(s_i, s_j^*) = P(s_i|s_j^*)P(s_j^*)$, where $P(s_0^*) = 1 - \Psi^*$ and $P(s_1^*) = \Psi^*$. Table 3 shows the whole set of joint and conditional probabilities. These expressions combined with the analytical models developed in Section 4.1 can be employed to characterise not only the average probability that a channel is observed as busy as a function of the DSA/CR user location and some basic primary signal parameters but also the joint and conditional probabilities that the channel is observed in any of its states with respect to the simultaneous observation of another node at a reference location.

Table 3 Joint and conditional probabilities of simultaneous observations.

s_i	s_j^*	$P(s_i, s_j^*)$	$P(s_i\|s_j^*)$
s_0	s_0^*	$(1 - P_{fa})(1 - \Psi^*)$	$1 - P_{fa}$
s_1	s_0^*	$P_{fa}(1 - \Psi^*)$	P_{fa}
s_0	s_1^*	$1 - \Psi - (1 - P_{fa})(1 - \Psi^*)$	$\frac{1 - \Psi - (1 - P_{fa})(1 - \Psi^*)}{\Psi^*}$
s_1	s_1^*	$\Psi - P_{fa}(1 - \Psi^*)$	$\frac{\Psi - P_{fa}(1 - \Psi^*)}{\Psi^*}$

5. Unified modelling approach

Spectrum usage models for the time (from both discrete- and continuous-time perspectives), frequency and space dimensions of spectrum usage have been reviewed in previous sections. In such models, each dimension of spectrum usage is characterised and modelled separately. This section discusses how the presented models could be combined and integrated into a unified modelling approach where the time, frequency and space dimensions of spectrum usage can simultaneously be taken into account and reproduced. The integration of the presented models is discussed in the context of analytical studies and simulation tools.

5.1. Integration of spectrum models in analytical studies

The models presented in this chapter are characterised by closed-form expressions describing relevant aspects and properties of spectrum usage, which can be employed in analytical studies of DSA/CR systems. Section 2.1 has presented deterministic and stochastic DC models to be combined with DTMCs. While the deterministic models are characterised by their particular mathematical expressions, the considered stochastic models (i.e., beta and Kumaraswamy distributions) are characterised by the corresponding PDFs/CDFs, which can be expressed in closed-form. Similarly, in Section 2.2 the suitability of various probability distributions to describe the statistical properties of busy and idle periods in real systems has been discussed. The mathematical expressions for the associated distributions can be employed in analytical studies as well. The time-correlation properties of spectrum usage have also been analysed in Section 2.3 and adequate mathematical expressions for the observed correlation patterns have been presented. In Section 3 it has been highlighted the existence of two important aspects to be accounted for in the frequency dimension of spectrum usage, namely the DC distribution over frequency, which can be characterised by means of beta and Kumaraswamy distributions, and the DC clustering over frequency, which can be described by means of a geometric distribution. The mathematical expressions for the associated distributions can be employed in analytical studies related to the frequency dimension of spectrum. Finally, the set of mathematical expressions provided in Section 4 can be used to characterise and predict not only the average level of spectrum occupancy (expressed in terms of the DC) but also the simultaneous observations that would be perceived by DSA/CR users at various geographical locations. An analytical study taking together into account aspects of various dimensions should rely on an adequate use and combination of the mathematical expressions associated to each dimension of spectrum usage (i.e., time, frequency and space). However, the concrete way in which such expressions should be combined and employed in an analytical study is a problem-specific aspect that depends on the particular scenario under consideration. It is worth noting that the availability of models capable to describe separately the relevant statistical properties of spectrum usage in its various dimensions is something that can facilitate and simplify their combination and joint use. If the relevant statistical properties of spectrum usage and their corresponding mathematical models are taken into account and adequately combined in the context of an analytical study, this would lead to more realistic and reliable results and conclusions.

5.2. Integration of spectrum models in simulation tools

Another important field of application of spectrum usage models is the development of simulation tools for the performance evaluation of DSA/CR networks and their associated techniques. Some simulation methods have already been provided in this chapter to illustrate the implementation of the presented models in simulation tools. This section provides a more detailed description of how the developed models can be combined and used together in order to generate artificial spectrum data capable to reproduce the statistical properties of spectrum usage in the time, frequency and space dimensions. It is worth noting that the procedure described in this section should not be interpreted as a dogmatic method but rather as an illustrative example. The spectrum usage models presented in this chapter could be combined and used together following other approaches. Moreover, some aspects of the simulation methodology proposed in this section are based on arbitrary decisions and might need some modifications in order to meet particular simulation needs. The main objective of this section is

to highlight the possibility to combine independent spectrum usage models into a unified simulation procedure that simultaneously takes into account all the considered aspects.

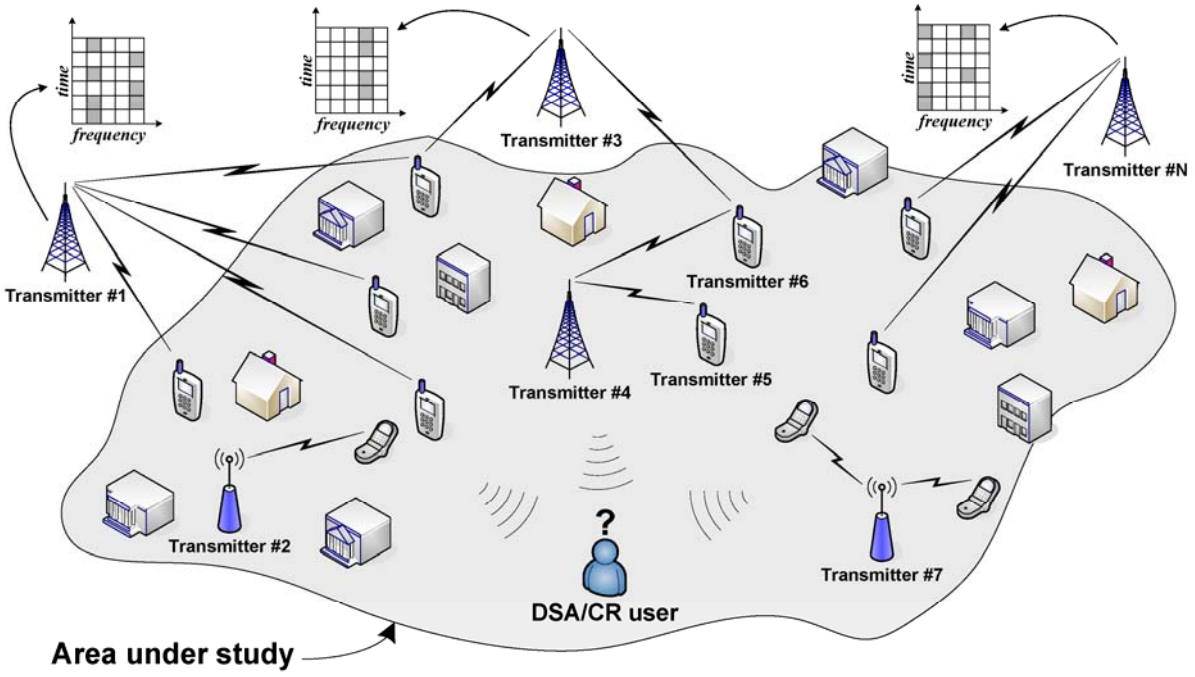

Figure 18 Generic simulation scenario.

A generic simulation scenario is shown in Figure 18. The considered simulation scenario assumes the presence of a number of primary transmitters over a certain geographical region. There exists a set of primary transmitters whose intended coverage areas overlap, totally or partially, with the considered geographical region. The activity of these primary transmitters needs therefore to be taken into account. Each primary transmitter is characterised by a certain location within the simulation scenario and a particular time-frequency transmission pattern as illustrated in Figure 18. The time-frequency pattern of each primary transmitter is defined by the set of radio channels over which the transmitter operates (note that a single primary transmitter may operate over several radio channels), the binary busy/idle occupancy sequence of each radio channel as well as the employed transmission powers. Notice that the transmission power may not be unique, for example, in the case of a time-slotted downlink channel where various slots are allocated to various receivers at different locations requiring different transmission powers. The objective is to determine the time-frequency pattern that would be perceived by a DSA/CR user over the whole spectrum band, at any arbitrary location within the simulated scenario, based on the time-frequency patterns of all primary transmitters.

A possible simulation method to generate artificial spectrum data based on the presented models is illustrated in Figure 19. The first step is to generate a time-frequency map of spectrum usage based on the simulation method described in Section 3.3. Such method is divided in three phases. The first two phases ensure that the generated spectrum data reproduce two relevant properties of spectrum usage in the frequency domain, namely the DC distribution (first phase of the algorithm) and the DC clustering (second phase of the algorithm). The third phase deals with the generation of individual busy/idle occupancy sequences for each of the radio channels within the considered spectrum band according to the average DC assigned to each channel as a result of the two previous phases. In this third phase, the simulation method described in Section 2.3.3.2 can be employed in order to reproduce not only certain specified statistical distributions for the lengths of busy and idle periods but also the desired time-correlation properties. The two-level modelling approaches presented in Section 2.2.3 can also be employed in conjunction with the simulation method of Section 2.3.3.2 in order to generate time-occupancy sequences with specific characteristics in the short- and long-terms, including the desired statistical distributions and time-correlation properties for busy and idle periods. The final result of the

aforementioned simulation methods is a single time-frequency map consisting of a time-domain binary occupancy sequence for each of the radio channels within the considered primary spectrum band. As an illustrative example, Figure 20 shows a time-frequency map of spectrum usage generated for the TETRA DL band along with the corresponding DC distribution over frequency. Figure 20 has been generated based on the simulation method of Section 3.3 (including the algorithm presented in Section 2.3.3.) and making use of the same configuration parameters employed to generate Figure 16.

The occupancy sequence observed in each radio channel of the obtained time-frequency map is the result of the activity pattern of at least one primary transmitter. The next step is to decide the primary transmitter(s) associated to each radio channel along with the corresponding location(s) and transmission power(s). These parameters can be selected so as to reproduce specific network deployments or in order to meet particular configurations or simulation needs. Another option is to select them randomly based on statistical spatial models. In the illustrative example of this section it is assumed that all radio channels belong to a single primary transmitter. Therefore, the location and transmission power associated to each channel is the same for all of them. The consequence of this simplistic assumption is that a change in the considered DSA/CR user location will result in the same SNR increase/reduction for all radio channels. In a more realistic configuration where different radio channels belong to various primary transmitters at different locations, a displacement of the DSA/CR user would result in approaching or moving away from various transmitters and hence different SNR increases/reductions for each radio channel. Although more realistic configurations are possible, this simple approach will suffice to illustrate the considered modelling approach.

The generated time-frequency map can be thought of as the superposition of the spectrum occupancy patterns of all the primary transmitters, where the individual occupancy sequence at each radio channel is indeed the transmission sequence of at least one primary transmitter. The next step is to decide the primary transmitter(s) associated to each radio channel along with the corresponding location(s) and transmission power(s). These parameters can be selected so as to reproduce specific network deployments or in order to meet particular configurations or simulation needs.

After generating the time-frequency map and selecting the primary transmitters, locations and transmission powers, the next step is to determine how the time-frequency map (i.e., the set of primary transmissions) is perceived by DSA/CR users at arbitrary locations within the area under study. This can be accomplished by means of the probabilities computed in Section 4.2, where the perceptions at arbitrary locations are determined based on the observations at one reference location where the receiving SNR is maximum. If the locations of the primary transmitters can be assumed to be known, then the simulation method is greatly simplified since (for each radio channel) the reference location is indeed the location of the primary transmitter (i.e., where the SNR is maximum) and the AF and reference DC values are identical (i.e., $\alpha = \Psi^*$) and equal to the average DC observed in the time-frequency map. The only unknown parameter is the average DC perceived at each location of interest, which can be computed based on the locations and transmission powers of the primary transmitters by making use of the expressions presented in Section 4.1.2. The time-frequency map perceived at every location can then be determined as follows: whenever the time-frequency map indicates a busy state, the channel may be observed as busy at an arbitrary location with probability $P(s_1|s_1^*)$ and whenever the map indicates an idle state, the channel may be observed as busy with probability $P(s_1|s_0^*)$. Following this procedure, the time-frequency map can be extrapolated to any arbitrary location within the area of study based on the corresponding conditional probabilities $P(s_i|s_j^*)$ provided in Table 3.

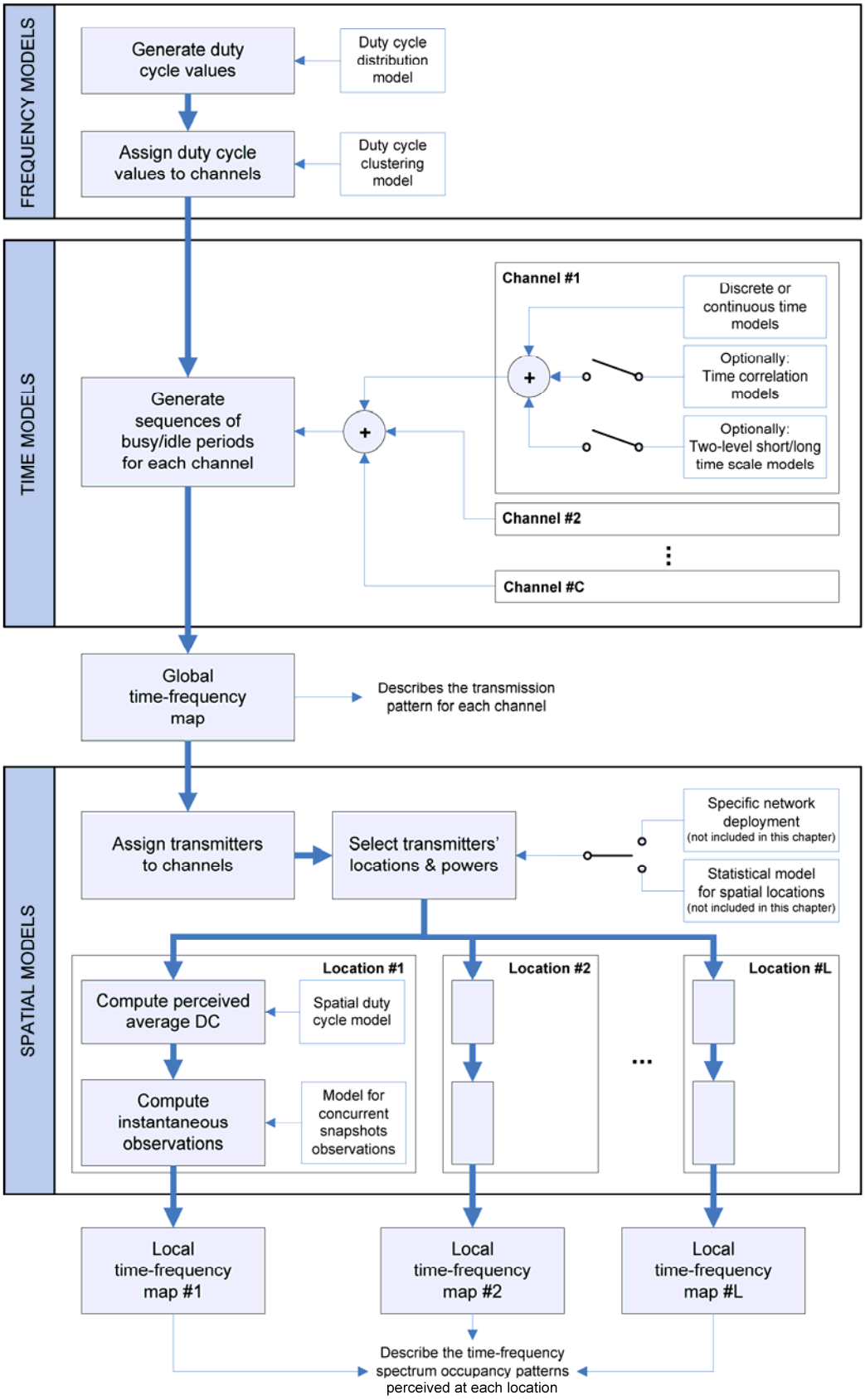

Figure 19 Unified simulation approach.

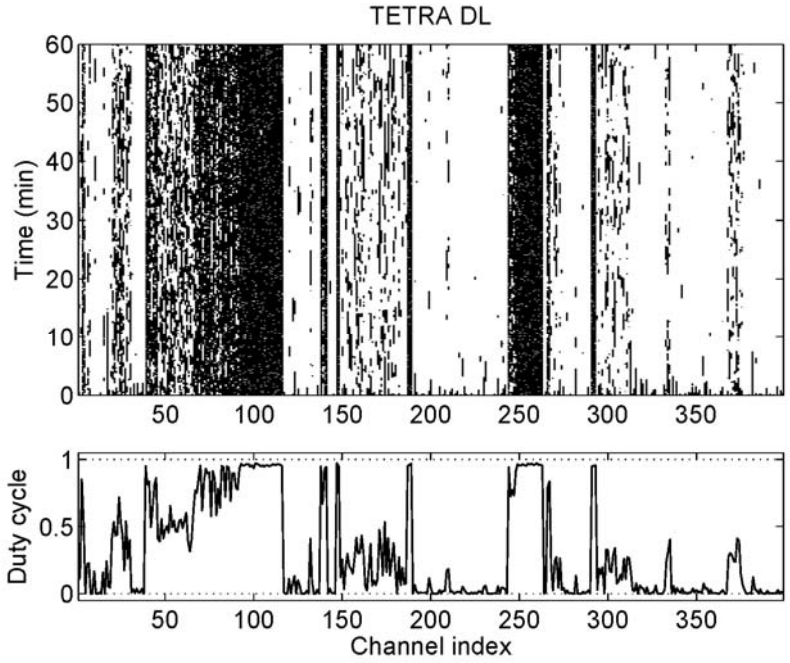

Figure 20 Time-frequency map of spectrum occupancy.

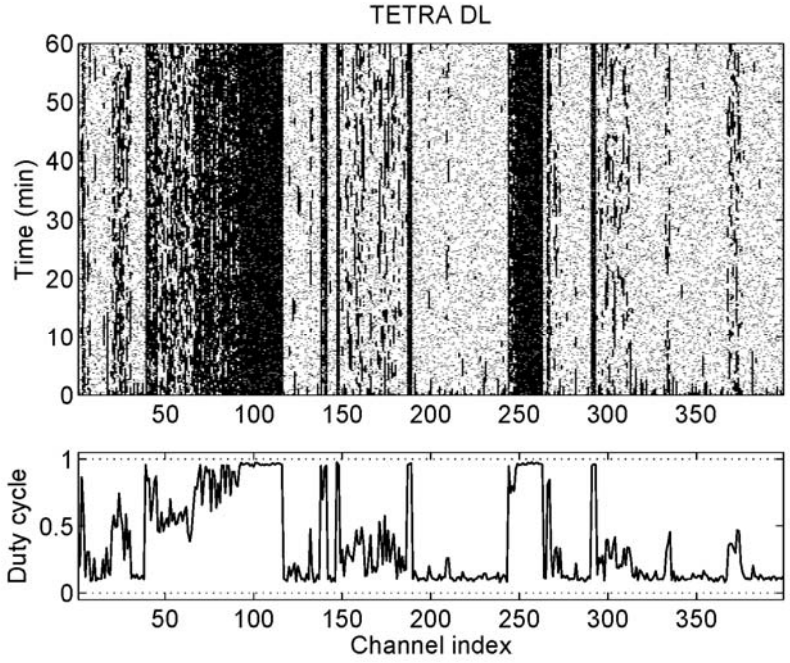

Figure 21 Time-frequency map of spectrum occupancy as perceived at 10-dB SNR.

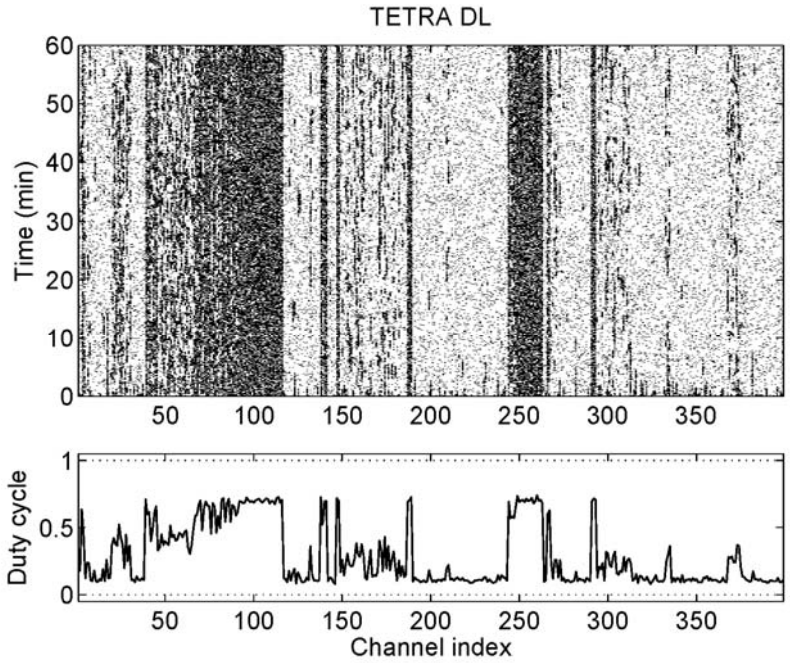

Figure 22 Time-frequency map of spectrum occupancy as perceived at 3-dB SNR.

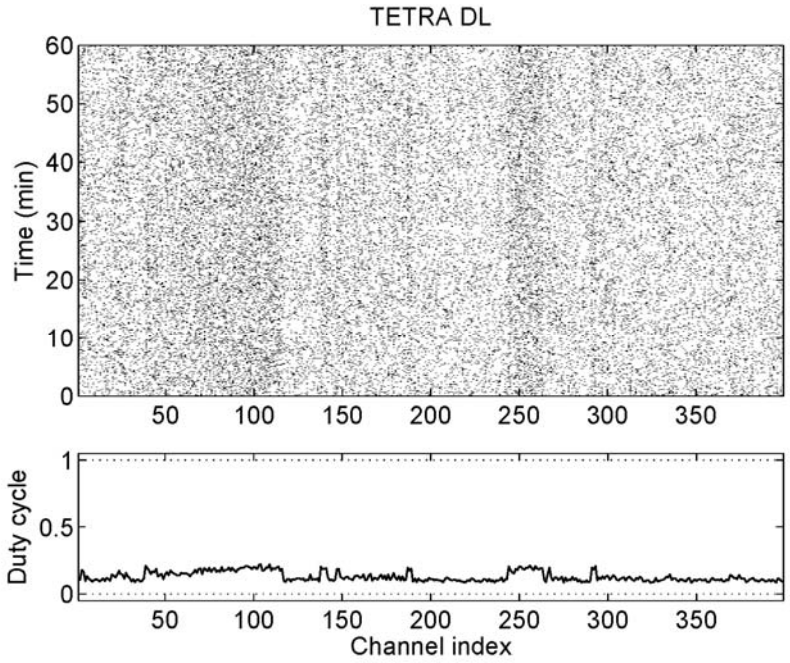

Figure 23 Time-frequency map of spectrum occupancy as perceived at 0-dB SNR.

As an example, Figure 21, Figure 22 and Figure 23 show the time-frequency map of Figure 20 as perceived at arbitrary locations where the receiving SNR is 10 dB, 3 dB and 0 dB, respectively. These results have been obtained assuming P_{fa} = 10% (the target P_{fa} has intentionally be set to this high value to clearly show its impact). As it can be appreciated in Figure 21, under high SNR conditions the channels are observed as busy whenever they are actually busy. However, there is an appreciable number of points indicating that, in some cases, the channel is detected as busy when it is actually idle. These points correspond to false alarms where the noise power of the receiver surpasses the decision threshold. In fact, while the DC shown in Figure 20 takes values within the interval [0,1], in Figure 21 it is above 10% (i.e., the P_{fa}). For locations where the experienced SNR is low, the primary signal may be received below the decision threshold, in which case it is misdetected. This is clearly shown in Figure 22 where the perceived DC is notably lower than in Figure 21. Finally, at locations with very low SNRs as in the example of Figure 23 the primary signals can hardly be detected and only false alarms are observed (i.e., $\Psi \approx P_{fa}$). It is worth noting in the examples of Figure 21, Figure 22 and Figure 23 that all channels experience a similar reduction of the DC as the SNR decreases because them all have been assumed to belong to the same primary transmitter. As mentioned above, in a more realistic scenario the DC may increase for some channels and decrease for some others at the same time as the DSA/CR user moves along the area under study.

The time-frequency maps observed at each location could be pre-computed off-line for a set of predefined locations within the simulated scenario (for example according to a regular grid) and loaded into the simulator during its initialisation. During the execution of the simulator, the location of each DSA/CR user can be approximated to the nearest location for which a time-frequency map has been pre-computed and, based on the associated map, the spectrum occupancy that would be perceived by each DSA/CR user can be determined. Another option is to implement the whole map generation method in the simulation tool and compute on-demand time-frequency maps during the execution as required. While the former approach may result in more efficient simulations and hence shorter execution times, the latter may provide more accurate results since the exact location of the DSA/CR user is employed instead of the closest point of a grid. However, both approaches would be valid in order to include in the simulations the statistical properties of spectrum usage observed for real radio communication systems in the time, frequency and space domains.

6. Conclusions

Spectrum models capable to capture and reproduce the relevant statistical properties of spectrum usage in real wireless communication systems play a key role in the practical development of the dynamic spectrum access/cognitive radio (DSA/CR) technology. The potential applicability of spectrum usage models ranges from analytical studies to the design and dimensioning of DSA/CR networks as well as the development of innovative simulation tools and more efficient DSA/CR techniques. Based on the particular set of statistical properties and features taken into account, spectrum models can be categorised into time-, frequency- and space-dimension models.

In the time domain, three important parameters need to be taken into account, namely the average channel occupancy level, which can be expressed in terms of the duty cycle (DC), the statistical distributions of the lengths of busy and idle periods, and the existing time-correlation structures. Spectrum usage can be modelled from discrete- and continuous-time perspectives. The stationary discrete-time Markov chain (DTMC) model widely used in the DSA/CR literature can reproduce the average occupancy level of a channel but it is not capable to reproduce more advanced features such as the distributions of busy and idle periods. However, a non-stationary DTMC modelling approach with appropriate deterministic and stochastic DC models can be employed to characterise not only the mean occupancy level but also the statistical properties of busy and idle periods observed in real-world channels. The continuous-time Markov chain (CTMC) model, another widely employed model, explicitly accounts for the lengths of busy and idle periods by assuming exponentially distributed state holding times. In general, however, the assumption of exponentially distributed busy and idle periods is invalid, meaning that the CTMC model is unrealistic. In real systems, other distributions result more adequate. At long time scales, the generalised Pareto distribution function can be appropriate for

various radio technologies, while at short time scales the most appropriate distribution is technology-dependent. A two-layer modelling approach combining the use of different models at long and short time scales has been presented as well as an adequate means to describe the spectrum occupancy patterns observed in real radio communication systems. The third relevant property (i.e., the time correlation structures) needs specific modelling and simulation approaches since the presented Markov chain models cannot capture and reproduce time-correlation properties.

The study of the joint time-frequency properties reveals three important aspects to be taken into account in spectrum usage modelling. First, the binary time-occupancy patterns of the channels belonging to the same spectrum band are mutually independent. Second, the DCs of the channels within the same spectrum band follow a beta/Kumaraswamy distribution. Third, the DC is clustered over frequency and the number of channels per cluster follows a geometric distribution. Based on these findings, a sophisticated procedure has been presented to generate artificial spectrum occupancy data for simulation and other purposes.

In the spatial dimension, spectrum usage can be characterised by means of a set models that describe the average spectrum occupancy level (expressed in terms of the DC) perceived by DSA/CR users at any geographical location based on the knowledge of the radio propagation environment and some simple primary signal parameters. An extension has also been presented that can be employed to characterise not only the average occupancy perception but also the simultaneous observations of various DSA/CR users on the spectrum occupancy pattern of the same transmitter.

Finally, the chapter has discussed how the proposed models can been combined and integrated into unified modelling approaches where the time, frequency and space dimensions of spectrum usage can simultaneously be taken into account and accurately reproduced. The presented models can be combined into a unified modelling approach to provide a complete and holistic characterisation of spectrum usage in real systems for the analysis, design and simulation of DSA/CR networks.

References

[1] D. Spaulding and G. H. Hagn, “On the definition and estimation of spectrum occupancy,” IEEE Transactions on Electromagnetic Compatibility, vol. EMC-19, no. 3, pp. 269–280, Aug. 1977.

[2] P. J. Laycock, M. Morrell, G. F. Gott, and A. R. Ray, “A model for HF spectral occupancy,” in Proceedings of the Fourth International Conference on HF Radio Systems and Techniques, 1988, pp. 165–171.

[3] M. López-Benítez, F. Casadevall, “An overview of spectrum occupancy models for cognitive radio networks,” Proceedings of the IFIP International Workshop on Performance Evaluation of Cognitive Radio Networks (PE-CRN 2011), May 13, 2011, pp. 1-10.

[4] O. C. Ibe, Markov processes for stochastic modelling, Academic Press, 2009.

[5] M. López-Benítez, F. Casadevall, “Empirical time-dimension model of spectrum use based on discrete-time Markov chain with deterministic and stochastic duty cycle models,” IEEE Transactions on Vehicular Technology, vol. 60, no. 6, pp. 2519-2533, Jul. 2011.

[6] Z. Wang and S. Salous, “Spectrum occupancy statistics and time series models for cognitive radio,” Journal of Signal Processing Systems, vol. 62, no. 2, pp. 145–155, Feb. 2011.

[7] D. Chen, S. Yin, Q. Zhang, M. Liu, and S. Li, “Mining spectrum usage data: a large scale spectrum measurement study,” in Proceedings of the 15th ACM Annual International Conference on Mobile Computing and Networking (MobiCom 2009), Sep. 2009, pp. 13–24.

[8] V. Blaschke, H. Jaekel, T. Renk, C. Kloeck, and F. K. Jondral, “Occupation measurements supporting dynamic spectrum allocation for cognitive radio design,” in Proceedings of the 2nd

International Conference on Cognitive Radio Oriented Wireless Networks and Communications (CrownCom 2007), Aug. 2007, pp. 50–57.

[9] A. Papoulis and S. U. Pillai, Probability, random variables, and stochastic processes, 4th ed. Boston: McGraw-Hill, 2002.

[10] P. Kumaraswamy, "A generalized probability density function for double-bounded random processes," Journal of Hydrology, vol. 46, no. 1-2, pp. 79–88, Mar. 1980.

[11] M. C. Jones, "Kumaraswamy's distribution: A beta-type distribution with some tractability advantages," Statistical Methodology, vol. 6, no. 1, pp. 70–81, Jan. 2009.

[12] S. Geirhofer, L. Tong, and B. M. Sadler, "A measurement-based model for dynamic spectrum access in WLAN channels," in Proceedings of the IEEE Military Communications Conference (MILCOM 2006), Oct. 2006, pp. 1–7.

[13] S. Geirhofer, L. Tong, and B. M. Sadler, "Dynamic spectrum access in WLAN channels: Empirical model and its stochastic analysis," in Proceedings of the First International Workshop on Technology and Policy for Accessing Spectrum (TAPAS 2006), Aug. 2006, pp. 1–10.

[14] S. Geirhofer, L. Tong, and B. M. Sadler, "Dynamic spectrum access in the time domain: Modeling and exploiting white space," IEEE Communications Magazine, vol. 45, no. 5, pp. 66–72, May 2007.

[15] L. Stabellini, "Quantifying and modeling spectrum opportunities in a real wireless environment," in Proceedings of the IEEE Wireless Communications and Networking Conference (WCNC 2010), Apr. 2010, pp. 1–6.

[16] M. Wellens, J. Riihijärvi, and P. Mähönen, "Empirical time and frequency domain models of spectrum use," Physical Communication, vol. 2, no. 1-2, pp. 10–32, Mar. 2009.

[17] T. Öztekin, "Comparison of parameter estimation methods for the three-parameter generalized Pareto distribution," Turkish Journal of Agriculture and Forestry, vol. 29, no. 6, pp. 419–428, Dec. 2005.

[18] M. López-Benítez, F. Casadevall, "Modeling and simulation of time-correlation properties of spectrum use in cognitive radio," Proceedings of the 6th International ICST Conference on Cognitive Radio Oriented Wireless Networks and Communications (CrownCom 2011), Jun. 2011, pp. 1-5.

[19] L. Devroye, Non-uniform random variate generation. Springer-Verlag, 1986.

[20] G. N. Tavares and A. Petrolino, "On the generation of correlated Gaussian random variates by inverse DFT," IEEE Transactions on Communications, vol. 59, no. 1, pp. 45–51, Jan. 2011.

[21] H. Hotelling and M. R. Pabst, "Rank correlation and tests of significance involving no assumption of normality," Annals of Mathematical Statistics, vol. 7, no. 1, pp. 29–43, Mar. 1936.

[22] M. López-Benítez, F. Casavadell, D. López-Pérez and A. V. Vasilakos, "Modeling and simulation of joint time-frequency properties of spectrum usage in cognitive radio," in Proceedings of the 4th International Conference on Cognitive Radio and Advanced Spectrum Management (CogART 2011), Invited Paper, Barcelona, Spain, October 2011, pp. 1-5.

[23] M. López-Benítez, F. Casadevall, "Spatial duty cycle model for cognitive radio," in Proceedings of the 21st Annual IEEE International Symposium on Personal, Indoor and Mobile Radio Communications (PIMRC 2010), Sep. 2010, pp. 1631-1636.

[24] T. Yücek and H. Arslan, "A survey of spectrum sensing algorithms for cognitive radio applications," IEEE Communications Surveys and Tutorials, vol. 11, no. 1, pp. 116–130, First Quarter 2009.